

# We are IntechOpen, the world's leading publisher of Open Access books Built by scientists, for scientists

4,800

Open access books available

122,000

International authors and editors

135M

Downloads

Our authors are among the

154

Countries delivered to

TOP 1%

most cited scientists

12.2%

Contributors from top 500 universities



WEB OF SCIENCE™

Selection of our books indexed in the Book Citation Index  
in Web of Science™ Core Collection (BKCI)

Interested in publishing with us?  
Contact [book.department@intechopen.com](mailto:book.department@intechopen.com)

Numbers displayed above are based on latest data collected.  
For more information visit [www.intechopen.com](http://www.intechopen.com)



# Thermoelectric Energy Harvesting: Basic Principles and Applications

Diana Enescu

## Abstract

Green energy harvesting aims to supply electricity to electric or electronic systems from one or different energy sources present in the environment without grid connection or utilisation of batteries. These energy sources are solar (photovoltaic), movements (kinetic), radio-frequencies and thermal energy (thermoelectricity). The thermoelectric energy harvesting technology exploits the Seebeck effect. This effect describes the conversion of temperature gradient into electric power at the junctions of the thermoelectric elements of a thermoelectric generator (TEG) device. This device is a robust and highly reliable energy converter, which aims to generate electricity in applications in which the heat would be otherwise dissipated. The significant request for thermoelectric energy harvesting is justified by developing new thermoelectric materials and the design of new TEG devices. Moreover, the thermoelectric energy harvesting devices are used for waste heat harvesting in microscale applications. Potential TEG applications as energy harvesting modules are used in medical devices, sensors, buildings and consumer electronics. This chapter presents an overview of the fundamental principles of thermoelectric energy harvesting and their low-power applications.

**Keywords:** thermal energy, Seebeck effect, thermoelectric generator, thermoelectric materials, design, low-power applications

## 1. Background about energy harvesting

Energy harvesting represents the energy derived from ambient sources that is extracted and directly converted into electrical energy. This way to provide energy is further used when another energy source is not available (off-grid use) to supply small- and medium-sized electronic devices, as well as electrical systems, with power from nW to hundreds of mW [1, 2]. Generally, energy harvesting refers to an environment with regular and well-assessed ambient energy sources. Energy harvesting is applied when there is a match between the available energy and the energy required.

Another term, *energy scavenging*, refers to an environment with strong non-uniform and unknown ambient energy sources [3]. Some examples of differences between the two terms are presented in **Table 1**.

The ambient energy sources used for energy harvesting are temperature gradient, electromagnetic radiation, light, motion and chemical energy (**Figure 1**).

	Scavenging	Harvesting
Thermal	Forest fires	Furnace covers
Photonic	Interior lighting	Diurnal solar cycles
Mechanical	Foot traffic	Motors, ductwork

**Table 1.**  
The difference between the terms “scavenging” and “harvesting” [3].

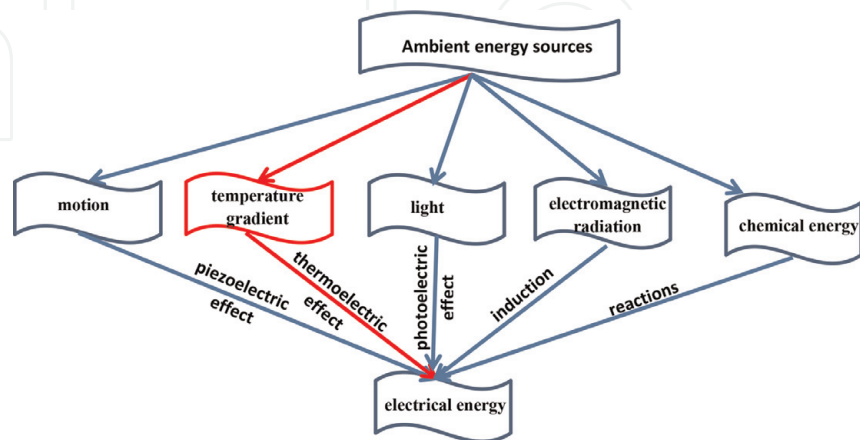


**Figure 1.**  
Energy harvesting sources.

An energy harvester consists of:

- an energy source (which is natural or artificial);
- one or more transducers that convert environmental energy into electrical energy;
- an energy storage device (e.g., a rechargeable battery or a capacitor that stores the harvested energy);
- process control electronics [4].

The most used energy harvesters are: thermal harvester based on the thermoelectric effect; light harvester based on the photoelectric effect; electromagnetic harvester based on induction; chemical harvester based on different reactions on the electrodes surfaces; piezoelectric harvester based on mechanical vibrations or human motion (which converts pressure or stress into electricity); radio-frequency (RF) harvester (that captures the ambient radio-frequency radiation).

Thermoelectric energy harvesting mainly depends on the operation of the thermoelectric generator (TEG). A TEG converts heat directly into electrical energy according to the Seebeck effect. In this case, the motion of charge carriers (electrons and holes) leads to a temperature difference across this device. Its operation is described in Section 2.3. Furthermore, the thermoelectric energy harvesting system can generate power from hundreds of  $\mu\text{W}$  to  $\text{mW}$  for different sensors and transmitters.

In the last decades, the specialists' attention has been focused on the development of green energy technology to decrease fossil fuel utilisation and greenhouse gas emissions. A thermoelectric harvester produces green energy for energy

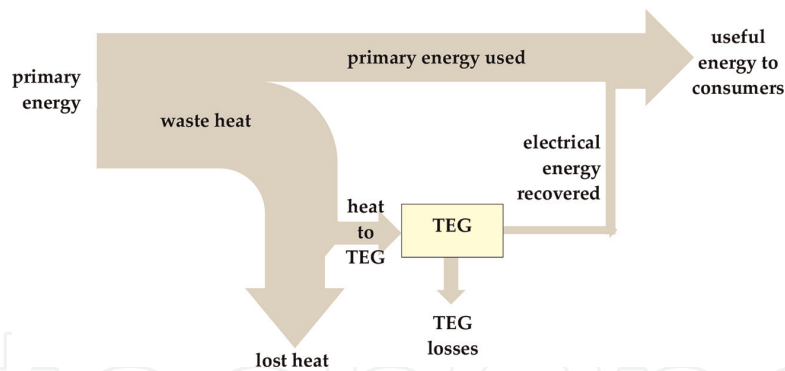


**Figure 2.**  
Electrical energy recovered from waste heat.

harvesting with a multitude of advantages: maintenance-free, because of the use of highly reliable and compact solid-state device; silent and quiet; highly efficient in environmental terms because the heat is harvested from waste heat sources and converted into electricity; operation with high maximum temperatures (up to 250°C); useful scalable applications configured to harvest wide amounts of energy when necessary; possibility to harvest power from both hot surface or cold surface; green energy behaviour, being eco-friendly [5]. A TEG device produces energy without using fossil fuel, leading to a reduction of greenhouse gas emissions.

Unlike thermodynamic PV systems or conventional heat engines (Rankine, Stirling), the energy conversion efficiency of the TEG is limited to about 5–15% [6]. The temperature difference across the TEG system and the dimensionless thermoelectric figure-of-merit ( $ZT$ ) have a major impact on the energy conversion efficiency [7]. It is desirable to obtain the maximum electric output power and efficiency when a TEG system operates. In case of waste heat recovery applications [8], only electric output power is significant and the heat not recovered is lost [9]. Considering that thermal energy harvesting has a reduced efficiency (5–6%), this could represent a major barrier for its extensive utilisation. An improvement in the TEG efficiency bigger than 10% has been lately obtained due to the progress of new thermoelectric materials [10].

The recovery of the electrical energy from waste heat using diverse sources is depicted in **Figure 2**.

## 2. Basic principles of thermoelectric energy generation

### 2.1 Thermoelectric effects

The thermoelectric effects are reversible phenomena leading to direct conversion between thermal and electrical energy [9]. Direct energy conversion relies on the physical transport properties of the thermoelectric materials (thermal conductivity, electric conductivity and Seebeck coefficient) and their energy conversion efficiency in terms of the figure-of-merit. These materials are suitable to convert thermal energy into electrical energy and vice-versa. The main phenomena that occur in a thermoelectric device are the thermoelectric effects (Seebeck, Peltier, Thomson), and the Joule effect.

- When the electrical energy is converted into thermal energy, the phenomenon is known as the *Peltier effect*, with applications in cooling and heating. The device used in such applications is called thermoelectric cooler (TEC) [11–13]. In this case, thermoelectric modules are efficient temperature controllers [14].

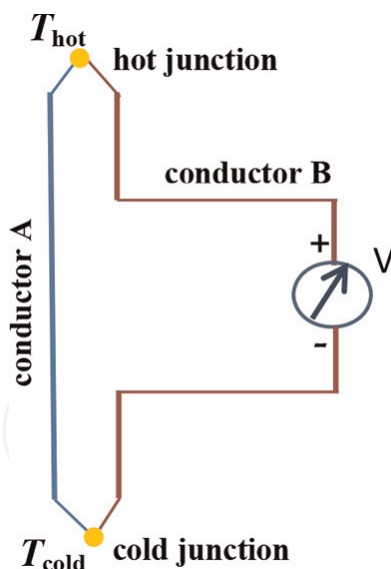


**Figure 3.**  
Schematic of the Seebeck effect in an open circuit.

- When the thermal energy is converted into electrical energy, the phenomenon is known as the *Seebeck effect*, with applications for power generation. The device used in such applications is called thermoelectric generator (TEG) [15, 16].

The *Seebeck effect* occurs when a temperature difference across a conductor provides a voltage at the conductor ends. Two distinct conductors A and B are linked together to compose the junctions of a circuit (**Figure 3**). These conductors are connected electrically in series and thermally in parallel. One junction has the hot temperature  $T_h$  and another one has the cold temperature  $T_c$ , with  $T_h$  bigger than  $T_c$ . The Seebeck effect appears due to the thermal diffusion which provokes the motion of the charge carriers (electrons or holes) across (or against) temperature difference in the conductors.

The Seebeck voltage at the circuit junctions can be written as:

$$V = \underbrace{(\alpha_A - \alpha_B)}_{\alpha_{AB}} \cdot \underbrace{(T_h - T_c)}_{\Delta T} \quad (1)$$

where  $\alpha_A$  and  $\alpha_B$  are the Seebeck coefficients for the conductors A and B, in  $V \cdot K^{-1}$ .

The Seebeck coefficient of a thermoelectric material or *thermopower*  $\alpha_{AB}$  is the connection parameter between the input temperature difference and the output voltage difference. The Seebeck coefficient of a thermoelectric material depends on temperature, as well as on other two physical transport properties (thermal conductivity, electric conductivity). It determines the thermoelectric material performance. Its magnitude ranges from  $\mu V \cdot K^{-1}$  to  $mV \cdot K^{-1}$  and depends on the junction temperature, and its sign is influenced by the semiconductor material [17]. Furthermore, the sign of the Seebeck coefficient depends on the type of carriers (electrons  $e^-$  and holes  $h^+$ ) conducting the electric current. If the electric current is conducted by  $e^-$ , the sign of the Seebeck coefficient is negative. If the electric current is conducted by  $h^+$ , the sign of the Seebeck coefficient is positive [18].

The Seebeck coefficient  $\alpha_{AB}$ , the temperature gradient  $\nabla T$ , and the electric field  $E$  are written under the following relationship:

$$\alpha_{AB} = \frac{E}{\nabla T} \quad (2)$$

The *Thomson effect* affirms that in any conductive material in which the electrical current flows in the presence of a temperature difference between two ends, heat is also released or absorbed. The Thomson heat released or absorbed is given as:

$$\dot{Q} = \underbrace{\rho \cdot J^2}_{\text{Joule heating}} - \underbrace{\mu_{AB} \cdot J \cdot \nabla T}_{\text{Thomson heating}} \quad (3)$$

where  $\rho = \frac{1}{\sigma}$  is the electrical resistivity in [ $\Omega \cdot \text{m}$ ],  $\sigma$  is the electrical conductivity in [ $\text{S} \cdot \text{m}^{-1}$ ],  $J$  is the current density in [ $\text{A} \cdot \text{m}^{-2}$ ],  $\mu_{AB}$  is the Thomson coefficient in [ $\text{V} \cdot \text{K}^{-1}$ ], and  $\nabla T$  is  $\nabla T = \frac{dT}{dx}$  is the temperature gradient along the conductor in [ $\text{K}$ ].

*Joule heating* occurs when an electric current that flows through a conductor produces heat. Joule heating does not change its sign in Eq. (3), while Thomson heating (the second term) changes its sign, following  $J$ .

Therefore, the sign convention of the Thomson coefficient is considered as [17]:

- *positive* when the current flows from the low-temperature side to the high-temperature side of the conductor and the heat is absorbed through it;
- *negative* when the current flows inversely and the heat is rejected from it;
- *null* when the current flows from the high to the low side and vice-versa and the heat is neither generated nor absorbed.

The following relationships hold between the Seebeck coefficient and the Peltier coefficient, as well as between the Seebeck coefficient and the Thomson coefficient. These are called Thomson relations [14]:

$$\pi_{AB} = \alpha_{AB} \cdot T \quad (4)$$

$$\mu_{AB} = T \cdot \frac{d\alpha_{AB}}{dT} \quad (5)$$

## 2.2 Thermoelectric effects and thermodynamic processes

Thermoelectric effects that take place in TEG devices are subject to the thermodynamic laws. According to thermodynamics, the heat transfer across a finite temperature difference is an irreversible process and the entropy change of such process is positive. The heat conduction and Joule heating are considered as irreversible processes.

The heat is irreversibly produced according to the Joule effect when an electrical current flows through a conductor or semiconductor. The Joule effect takes place at the TEG interconnects due to their electrical contact resistance or in a thermocouple. Other irreversibilities are found in the heat transfer between the TEG and the local environment [9]. If the irreversible processes are removed, the entropy becomes null. In this case, the ideal conditions given by the Carnot efficiency or *COP* (coefficient of performance) are achieved [19]. A deep overview of steady-state irreversible processes as heat conduction in semiconductor materials, metals and other solid-state devices is presented in [19, 20]. The Seebeck, Thomson and Peltier effects are reversible thermodynamic processes [21]. When the current flows through a conductor, both the Joule effect and the Thomson effect take place



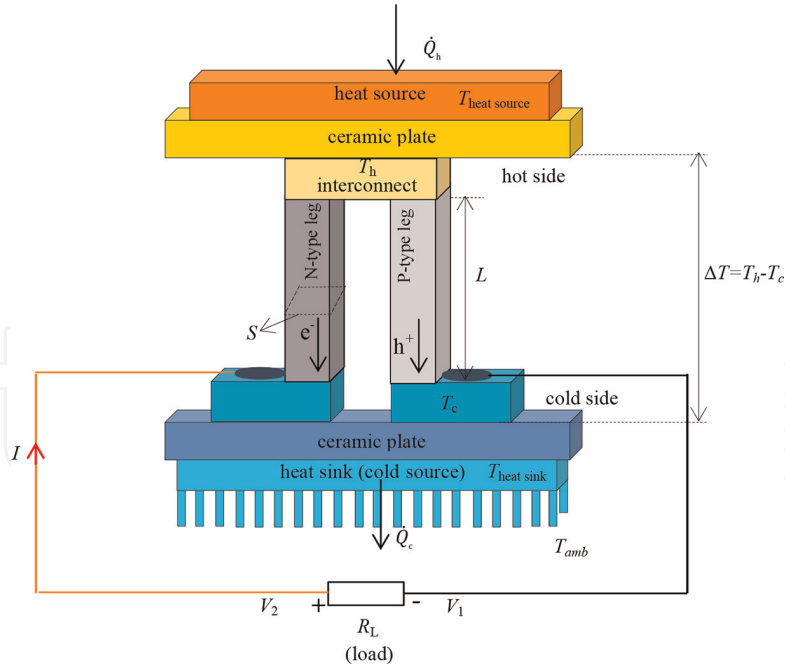


**Figure 4.**  
Schematic of a TEG device with a single thermoelectric couple and two legs.

simultaneously, and the magnitude of the Thomson effect is about two times less than the magnitude of the Joule effect [17].

### 2.3 TEG structure and model

The TEG device is composed of one or more thermoelectric couples. The simplest TEG consists of a thermocouple, comprising a pair of P-type and N-type thermoelements or legs connected electrically in series and thermally in parallel. The differentiation between N- and P-doped materials is important. The P-type leg has a positive Seebeck coefficient and an excess of holes  $h^+$ . The N-type leg has a negative Seebeck coefficient and an excess of free electrons  $e^-$  [22]. The two legs are linked together on one side by an electrical conductor forming a junction or interconnect, usually being a copper strip. Let us denote the voltage at the outside terminal connected to the N-type leg on the cold side of TEG as  $V_2$ , while the voltage at the external terminal connected to the P-type leg on the cold side of TEG is  $V_1$  (**Figure 4**). An electrical load having resistance  $R_L$  is connected in series with the output terminals of TEG creating an electric circuit. When the electric current flows in this electrical load, an electrical voltage is generated at its terminals. The TEG device will generate DC electricity as long as there is a temperature gradient between its sides. When the temperature difference  $\Delta T = T_h - T_c$  across the TEG device increases, more electric output power will be generated.

A number of thermoelectric couples  $n$  form a TEG system wired electrically in series and sandwiched between two ceramic plates to maximise the output voltage from the TEG (**Figure 5**).

In this case, the equivalent internal resistance of the thermoelectric couples in series is:

$$R = n \cdot \left[ \rho_P \cdot L_P \cdot (S_P)^{-1} + \rho_N \cdot L_N \cdot (S_N)^{-1} \right] \quad (6)$$

and the equivalent thermal conductance of the thermoelectric couples in parallel is:

$$K = n \cdot \left[ k_P \cdot S_P \cdot (L_P)^{-1} + k_N \cdot S_N \cdot (L_N)^{-1} \right] \quad (7)$$

where  $\rho = R \cdot \frac{S}{L}$  is the electrical resistivity of each leg,  $S$  is the cross-sectional area of the each leg in  $[\text{m}^2]$ ,  $L$  is the leg length in  $[\text{m}]$ ,  $k$  is the thermal conductivity of each leg in  $[\text{W} \cdot (\text{m} \cdot \text{K})^{-1}]$ , and the thermal conductance of each leg is  $K = k \frac{S}{L}$  in  $[\text{W} \cdot \text{K}^{-1}]$

These relations are further simplified considering that N-type and P-type legs are the same as form ( $L = L_P = L_N$  and  $S = S_P = S_N$ ) and material properties ( $\rho = \rho_P = \rho_N$ , and  $k = k_P = k_N$ ). The equivalent internal resistance becomes:

$$R = n \cdot 2\rho \cdot L \cdot (S)^{-1} \quad (8)$$

and the equivalent thermal conductance is:

$$K = n \cdot 2k \cdot S \cdot (L)^{-1} \quad (9)$$

If the electrical contact resistance  $R_a$  is not negligible, the equivalent internal resistance of the thermoelectric couples in series becomes:

$$R = n \cdot 2\rho \cdot L \cdot (S)^{-1} + R_a \quad (10)$$

The voltage at the TEG terminals is:

$$V_{\text{TEG}} = V_2 - V_1 = n \cdot (I \cdot R - \alpha_{\text{PN}} \cdot \Delta T) = n \cdot I \cdot R - V_{\text{Seebeck}} \quad (11)$$

where  $\alpha_{\text{PN}} = (\alpha_P - \alpha_N)^2$  is the Seebeck coefficient of the thermoelectric couple. The input electrical current in the circuit is:

$$I = \frac{V_{\text{Seebeck}}}{n \cdot R + R_L} = \frac{n \cdot \alpha_{\text{PN}} \cdot \Delta T}{n \cdot R + R_L} \quad (12)$$

where the load resistance  $R_L$  is connected to the output of the circuit where the electric output power generated by TEG is consumed; the Seebeck voltage is  $V_{\text{Seebeck}} = V_P - V_N = \alpha_{\text{PN}} \cdot \Delta T$ . The relationship between  $V_{\text{Seebeck}}$  and  $\Delta T$  is non-linear, therefore  $\alpha_{\text{PN}}$  depends on temperature.

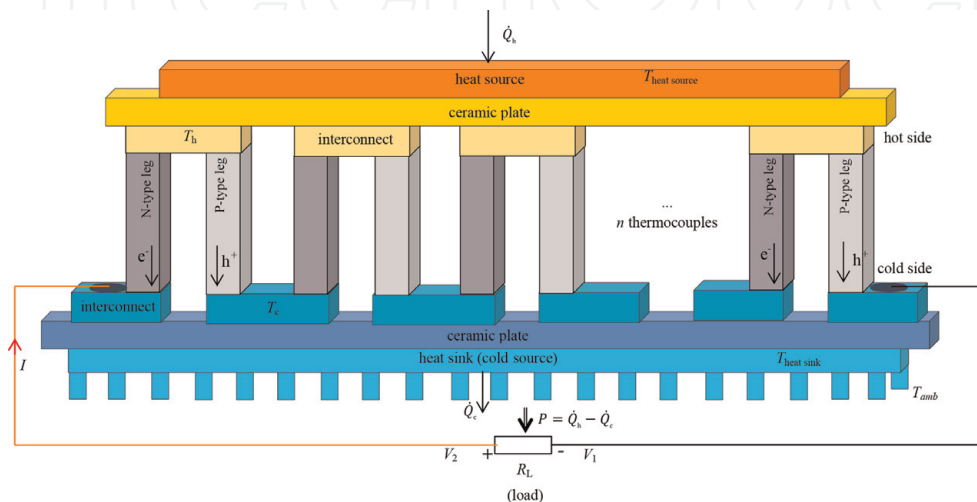


**Figure 5.**  
 Schematic of a TEG device with  $n$  thermoelectric couples.



The electric output power delivered by TEG to the load is:

$$P = n \cdot (\alpha_{PN} \cdot I \cdot \Delta T - R \cdot I^2) \quad (13)$$

On the other side, the electric output power absorbed by the load (considering the conventional sign, with the current flowing as indicated in **Figure 5**) is:

$$P = -V_{TEG} \cdot I = n \cdot (R \cdot I^2 - \alpha_{PN} \cdot I \cdot \Delta T) \quad (14)$$

The electric output power absorbed by the load resistance  $R_L$  is:

$$P_R = I^2 \cdot R_L = \left( \frac{n \cdot \alpha_{PN} \cdot \Delta T}{n \cdot R + R_L} \right)^2 \cdot R_L \quad (15)$$

The maximum electric output power of a TEG is obtained when the electrical output power is maximised with respect to the electric current:

$$P_{\max} = n \cdot \frac{(\alpha_{PN} \cdot \Delta T)^2}{4R} \quad (16)$$

$$I_{\max} = \frac{\alpha_{PN} \cdot \Delta T}{2R} \quad (17)$$

The maximum electrical output power delivered by TEG is obtained if the load resistance is equal to the equivalent internal resistance of the thermoelectric couples in series ( $R_L = R$ ) [23].

The heat flow rate absorbed at the hot junction of the TEG depends on the Peltier heat, the heat conduction and the Joule heat. The heat flow rate absorbed at the hot junction depends on the thermoelectric material properties and leg geometries:

$$\dot{Q}_h = n \cdot \left[ \alpha_{PN} \cdot T_h \cdot I - \frac{R \cdot I^2}{2} + K \cdot \Delta T \right] \quad (18)$$

A TEG could be considered as a thermal battery, a physical structure used to store and release thermal energy. The electromotive force of this thermal battery is the Seebeck voltage (**Figure 6**).

## 2.4 Components of a thermoelectric energy harvesting system

A thermoelectric energy harvesting system consists of the following parts (**Figure 7**):

- *Thermoelectric generator* (TEG): if  $\Delta T$  is kept between the hot and cold sides of the device, an external circuit can be supplied by the voltage resulting at the TEG output terminals, providing power to the external electrical load. A single TEG generates power from 1 to 125 W. The use of more TEGs in a modular connection may increase the power up to 5 kW and  $\Delta T_{\max}$  could be bigger than 70°C.
- *Heat source*, for example, a heat pipe system (the TEG devices and the heat pipe system can be used together in waste heat recovery systems). The heat pipe is a passive (no moving parts or fan) metallic device which has a high heat transfer capacity (very high thermal conductivity), with minimal thermal resistance and almost no heat loss; it operates in a medium temperature to high-temperature range; the common working fluid is water operating at a

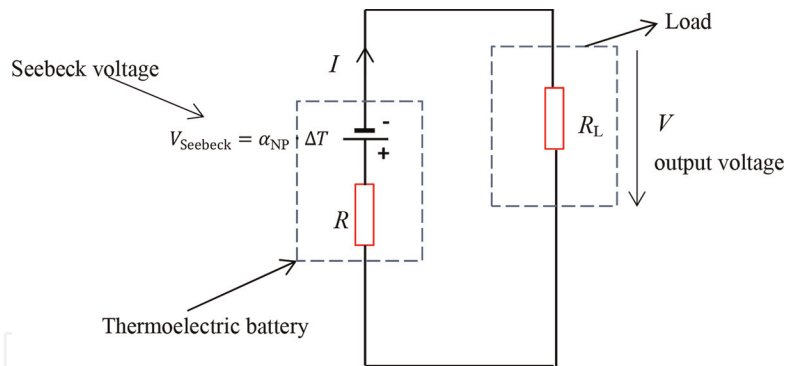


**Figure 6.**  
 Equivalent circuit of a TEG device.

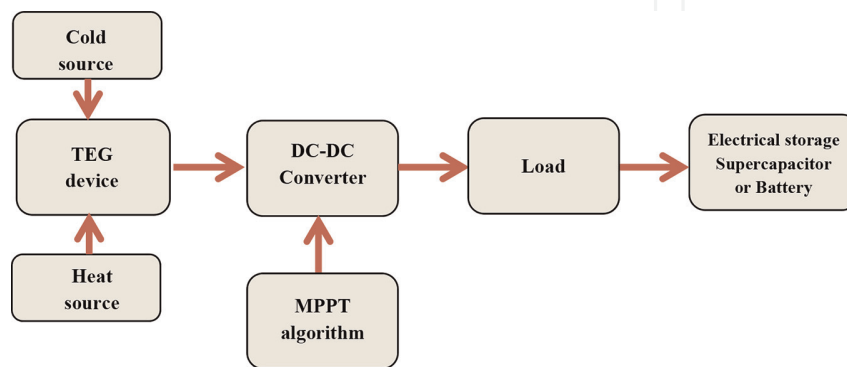


**Figure 7.**  
 Block diagram of a thermoelectric energy harvesting system.

temperature of about 300°C; for higher operating temperature ranges other working fluids are used (e.g., naphthalene or liquid metals like potassium and sodium) [24]; heat pipes are used for temperature regulation of the TEGs; in some applications (e.g., industrial glass processes) a heat exchanger can be attached on the hot side; its role is to absorb the thermal energy (e.g., from the glass process exhaust stream) and to transfer it to the TEG, which converts it partially into electrical energy; the remaining unconverted thermal energy is transferred from the TEG cold side to the cold source, and is dissipated to the environment at ambient temperature  $T_{amb}$ .

- *Cold source* is the heat transfer system containing heat exchangers (heat sinks, coils, cooling blocks and radiators) to enhance the heat dissipation across the TEG; this process is useful to obtain a bigger temperature difference across the TEG [7, 25]; the heat sink is a device that has the role to transfer heat from a hot surface to a fluid (gas, ambient air or liquid); the assessment and design of different heat sink types for TEG system is presented in [26]. The metal heat sink contains many fins. To increase its dissipation rate, the fins area, the heat transfer coefficient, and the fin thermal conductivity are raised.

The heat sink is required at the TEG when a high heat flow rate is applied on the TEG hot side, and the cold side is kept at low temperature, leading to high conversion efficiency; in this case, the TEG efficiency is strongly influenced by the TEG design.

- *DC-DC converter* (Boost, Buck-Boost, Buck, Sepic, or Cuk converter), which is a power electronic circuit designed for voltage conversion (to convert a DC source from one voltage level to another voltage level) [27]; since the output

voltage of the TEG is low or is not constant, it is necessary to provide a DC-DC converter; its role is to increase the output voltage obtained in the TEG (which depends on the number of TEGs in series and on the TEG features) corresponding the requirements of the external load. For these DC-DC converters, accurate control is necessary. In this case, the implementation of the Maximum Power Point Tracking (MPPT) algorithm within the DC-DC converter controller is essential. To enhance the real system feasibility, it is necessary to harvest from TEGs as much electric output power as possible; the effectiveness of TEG operation could be checked by assessing the DC-DC converter operation and the MPPT control.

- *DC load*, used to be connected to a supercapacitor or to recharge a battery to store energy; the battery stores DC voltages at a charging mode and powers DC electrical energy in a discharging mode; typical DC loads for TEG like batteries operate at 12 V; the output voltage of the TEG device at the MPP (Maximum Power Point) must be higher than 12 V for example in buck converter applications [27]; to avoid the battery overcharging a battery regulator is sometimes used; the electric power output from the DC-DC converter can be stored over time in a supercapacitor, to be released to the load when needed [28].

The efficiency of the thermoelectric energy harvesting system is defined as the ratio of the electrical energy output (used or stored) to the total energy input. This efficiency also contains the electrical efficiency of TEGs, the heat exchangers efficiency, as well as the efficiency of the DC-DC converter. The total energy input especially depends on the energy obtained from the hot source. Also, the total energy input depends to a lesser extent on the mechanical energy needed to operate the thermoelectric energy harvesting system (e.g., pressure losses in the heat exchangers or cooling of the cold heat sink) [29].

Researchers are focused on the improvement of the thermoelectric conversion efficiency of TEGs. For this reason, two objectives must be fulfilled. The first objective is to improve the dimensionless figure-of-merit  $ZT$  by the optimisation of thermoelectric materials. The second objective is to decrease the thermal resistance between the heat source and the hot side of the TEG, as well as between the cold side of the TEG and the environment [30].

## 2.5 Efficiency assessment of a TEG device

The electrical efficiency of a TEG (or thermoelectric conversion efficiency) is the ratio between the electric output power  $P$  delivered to the load and the rate of heat input  $\dot{Q}_h$  absorbed at the hot junction of the TEG and transferred through the TEG. This means that a TEG converts the rate of heat input  $\dot{Q}_h$  into electric output power  $P$  with electrical efficiency  $\eta_{\text{TEG}}$  [5].

$$\eta_{\text{TEG}} = \frac{P}{\dot{Q}_h} \quad (19)$$

Eq. (19) is written in more details as

$$\eta_{\text{TEG}} = \frac{n \cdot R_L \cdot \Delta T \cdot \alpha_{\text{PN}}^2}{K \cdot (n \cdot R + R_L)^2 + n \cdot (R_L \cdot T_h + n \cdot R \cdot T) \cdot \alpha_{\text{PN}}^2} \quad (20)$$

where  $T$  is the absolute temperature representing the mean temperature between the cold side and hot side of the TEG and is written as  $T = \frac{T_h + T_c}{2}$ .

The efficiency corresponding to  $P_{\max}$  is:

$$\eta_{\text{TEG}} = \frac{\Delta T}{4 \cdot Z^{-1} + T_h + T} \quad (21)$$

where  $Z = \frac{\alpha_{\text{PN}}^2}{K \cdot R}$  is the figure-of-merit for a thermocouple.

The thermoelectric conversion efficiency is maximised with respect to  $R_L$  [23] when

$$m = \frac{R_L}{R} = \sqrt{1 + ZT} \quad (22)$$

The TEG device operates as all thermal engines with efficiency less than the efficiency of ideal Carnot cycle  $\eta_C = \frac{T_h - T_c}{T_h} = \frac{\Delta T}{T_h} < 1$  [31]:

$$\eta_{\text{TEGmax}} < \eta_C \quad (23)$$

In this case, the thermoelectric conversion efficiency is limited by the Carnot efficiency and is written, by introducing the reduced efficiency  $\eta_r$ , as:

$$\eta_{\text{TEGmax}} = \underbrace{\frac{\sqrt{1 + ZT} - 1}{\sqrt{1 + ZT} + \frac{T_c}{T_h}}}_{\eta_r} \cdot \underbrace{\frac{\Delta T}{T_h}}_{\eta_C} = \frac{m - 1}{m + \frac{T_c}{T_h}} \cdot \frac{\Delta T}{T_h} = \frac{\eta_r}{T_h} \cdot \Delta T \quad (24)$$

and the corresponding electric output power is:

$$P(\eta_{\text{TEGmax}}) = \frac{n \cdot \sqrt{1 + ZT}}{R} \cdot \left( \frac{\alpha_{\text{PN}} \cdot \Delta T}{\sqrt{1 + ZT}} \right) \quad (25)$$

For a cold side temperature of  $T_c = 300$  K and  $\Delta T$  in the range of 20 K,  $\eta_{\text{TEGmax}} \cong 1\%$  is obtained [32].

As observed in Eq. (24), the TEG efficiency strongly depends on the *operating temperatures* of TEG ( $\Delta T$  between the junctions), the *dimensionless thermoelectric figure-of-merit*  $ZT$ , and additionally the TEG *design* (cross-sectional area, length and shape) [33].

The TEG efficiency  $\eta_{\text{TEG}}$  rises almost linearly with  $\Delta T$ , and the ratio  $\frac{\eta_r}{T_h}$  is almost constant [5]. The bigger the temperature difference, the more efficient the TEG device will be. A TEG can work at about 20% of the Carnot efficiency over a large temperature range [24]. The TEG efficiency is about 5% and its electric output power is delivered at any  $\Delta T$ . If materials with  $ZT = 10$  would exist, there could be TEGs with  $\eta_{\text{TEG}} = 25\%$  at  $\Delta T = 300$  K [25].

The thermoelectric waste heat recovery is influenced to a bigger extent by the thermoelectric conversion efficiency  $\eta_{\text{TEG}}$ , and to a lesser extent by the heat exchanger design. The ratio between thermal efficiency  $\eta_t$  and thermoelectric conversion efficiency represents the fraction of waste heat passed through the thermoelectric couples, given as [34]:

$$\varepsilon = \frac{\eta_t}{\eta_{\text{TEG}}} \quad (26)$$

The maximum efficiency  $\eta_{\text{TEGmax}}$  depends on the temperature difference  $\Delta T_{\text{TEG}}$  at which the TEG works [31]. The maximum conversion efficiency occurs when:

$$\frac{R_L}{R} = \sqrt{1 + Z \frac{T_c + T_h}{2}} \quad (27)$$

### 2.5.1 The dimensionless thermoelectric figure-of-merit $ZT$

The dimensionless thermoelectric figure-of-merit  $ZT$  is used to characterise a thermoelectric material performance, as well as the efficiencies of various TEGs working at the same temperatures [24].

$ZT$  depends on the physical transport properties: the thermal conductivity  $k$ , the electrical conductivity  $\sigma = \frac{1}{\rho}$ , and the Seebeck coefficient  $\alpha$ :

$$ZT = \frac{\alpha^2 \cdot T}{\rho \cdot k} = \frac{\alpha^2 \cdot \sigma \cdot T}{k} \quad (28)$$

The upper side term  $\alpha^2 \cdot \sigma$  is called *the power factor*, a parameter that assesses the performance of a thermoelectric material.

The higher is  $ZT$ , more performant is the thermoelectric material and the better is the TEG. In the practical applications, the maximum  $ZT$  is about 2 and corresponds to a maximum conversion efficiency of about 20% [35].

A good thermoelectric material must fulfil the following requirements:

- Seebeck coefficient as high as possible to maximise energy conversion; the generated open-circuit-voltage is proportional to the Seebeck coefficient and to the temperature difference across the TEG ( $V_{\text{Seebeck}} = \alpha_{\text{PN}} \cdot \Delta T$ ). In this case, a high Seebeck coefficient leads to a high voltage. This condition is very important for increasing the energy conversion [22].
- Electrical conductivity  $\sigma$  as high as possible in order to reduce Joule heating due to the internal electrical losses [22].
- Thermal conductivity  $k$  as low as possible to maintain heat at the junctions, to allow a large  $\Delta T$  maintained across the TEG, and to minimise thermal losses through the thermoelectric material [19].

The effective figure-of-merit of TEG,  $ZT_{\text{TEG}}$  depends on the dimensionless thermoelectric figure-of-merit, and the specific contact electrical resistivity according to the expression:

$$ZT_{\text{TEG}} = \frac{L}{(L + 2\sigma \cdot \rho_a)} \cdot ZT = \frac{L}{(L + 2\sigma \cdot \rho_a)} \cdot \frac{\alpha^2 \cdot \sigma \cdot T}{k} \quad (29)$$

where  $\rho_a = R_a \cdot S_a$  is the specific contact electrical resistivity. Ideally, for an efficient TEG  $\rho_a < 1\mu\Omega \cdot \text{cm}^2$  and instead, for a typical TEG,  $\rho_a < 2 \cdot 10^{-4}\Omega \cdot \text{cm}^2$  [36].

Although the low efficiency is a drawback to the progress of TEGs, researchers' and manufacturers' attention is focused on the improvement of the following characteristics:

- the dimensionless thermoelectric figure-of-merit  $ZT$ ;



- the operating range of thermoelectric materials to work with the  $\Delta T$  as high as possible;
- the use of low-price materials to reduce the negative impact of low efficiency [29].

The most popular thermoelectric material is Bismuth Telluride ( $\text{Bi}_2\text{Te}_3$ ). Its utilisation in TEGs is limited (only for industrial modules with an average value of  $ZT$  from 0.5 to 0.8) because the maximum temperature at the hot side of the devices is relatively reduced [29]. In the power generation applications, the best commercially available TEGs made of  $\text{Bi}_2\text{Te}_3$  have a  $ZT$  of about 1 at the temperature 300 K, leading to a low thermal efficiency of the thermoelectric device (less than 4%) [24]. The thermoelectric materials must be both stable from the chemical point of view and strong from the mechanical point of view at high temperatures (e.g., for the automotive exhaust waste heat recovery, at specific working conditions, the range of the average exhausts temperature is from 500 to 600°C with values increasing up to 1000°C) [37]. To improve the thermoelectric properties of TEG, the researchers' attention is focused on the development of new thermoelectric materials. Calcium manganese and lead telluride are the thermoelectric materials used in the TEG legs, because they resist at higher temperatures. The hot side of TEG is made of materials having a high  $ZT$  at higher temperatures (e.g., lead telluride). The cold side of the TEG is made of materials having high  $ZT$  at reduced temperatures (e.g.,  $\text{Bi}_2\text{Te}_3$ ) [24]. At present, even though the research of the thermoelectric materials development is focused on obtaining the high  $ZT$  of 2, unfortunately the efficiency of TEG is limited to  $\eta_{\text{TEG}} < 10\%$  [38]. Significant progress has been made towards increasing the thermoelectric efficiency of different inorganic material classes (e.g., skutterudites [39], tellurides [40, 41], half-Heuslers [42] and silicides [43]). The researchers' attention is focused on the development of organic materials for thermoelectric energy harvesting due to their advantages (e.g., low-cost, reliability, low weight and so on). For this reason, some polymers with different doping levels (like polyaniline (PANI), polyamide (PA), and poly (3,4-ethylenedioxythiophene) or PEDOT) are assessed for future applications [44].

To obtain high efficiency, segmented TEGs use high-temperature differences to raise the Carnot efficiency  $\eta_C$  [45]. When a TEG operates with a high-temperature difference, each thermoelement of the device can be divided into multiple segments of different thermoelectric materials. In this way, each material is working in a more limited temperature range where this has a good performance [46]. The segmented design of a TEG is an efficient mode to improve its performance. In this case, two or more thermoelectric materials along the direction of the leg height are used to match the optimal temperature range of the thermoelectric material. It means that a thermoelectric material with high efficiency at raised temperature is segmented with another thermoelectric material with high efficiency at reduced temperature [45]. The maximum efficiency is obtained when the relative current density  $\bar{j}$  is equal to the compatibility factor  $u$  of the thermoelectric material [47]:

$$\underbrace{\frac{J}{k \cdot \nabla T}}_{\bar{j}} = \underbrace{\frac{\sqrt{1 + ZT} - 1}{\alpha \cdot T}}_u \quad (30)$$

The compatibility factor is used for choosing the proper material [48]. El-Genk and Sabre [46] obtained a TEG energy conversion efficiency of about 12% by using a segmented thermoelectric couple. Snyder [47] observed that the segmentation of



the thermoelements with SnTe or PbTe produced low extra power, while the filled Skutterudite obtained an increment in efficiency from 10.5 to 13.6%. Further studies [47, 48] reported that the segmentation was efficient only for  $u \leq 2$ . Ngan et al. [49] demonstrate that segmentation reduces the total efficiency by neglecting the compatibility factor of thermoelectric materials. Hung et al. [50] showed that the performance and the power production of the segmented TEG are three times bigger than a normal TEG. The analytical assessment concerning the effect of the leg geometry on the performance of the segmented TEG was performed in [51, 52]. Their conclusion is that both power and efficiency are increased when the segmented TEG is used. Vikhor and Anatyshuk [53] carried out a theoretical analysis. The results showed an efficiency of the segmented TEGs bigger than 15% compared to the non-segmented TEGs. Zhang et al. [54] proposed a design method of optimization with predictive performance to obtain maximum conversion efficiency. In this case, the segmented modules consisted of Bi<sub>2</sub>Te<sub>3</sub>-based alloys and CoSb<sub>3</sub>-based skutterudites, with an efficiency of 12% when working under a  $\Delta t = 541^\circ\text{C}$ . The very low losses and the good design based on the numerical evaluation showed that the conversion efficiency was up to 96.9% of the theoretical efficiency.

### 2.5.2 TEG design for energy harvesting applications

In TEG systems, a crucial factor is the optimisation of the systems design, together with the heat source and heat sink attached to the TEG device. Industrial utilisation of TEGs needs other components (like heat exchangers and DC-DC converter) to form a powerful TEG [29].

The TEG performance is influenced not only by the low conversion efficiency, but also by the heat transfer conditions on the cold and hot sides of TEG and its geometry. The  $\Delta T$  between two junctions depends on the good heat transfer between TEGs and heat sources or heat sinks. For this reason, the design and interactions between heat exchangers and TEGs are very important problems. There are two paths to solve these problems together. The first path is the optimisation of the TEGs system. The second path is the enhancement of the heat transfer at the TEG sides [55].

#### 2.5.2.1 Optimization of the TEG device

The TEG device optimisation is correlated with the impact of the geometry device [56]. It has been demonstrated that an important rise in the electric output power from TEG is obtained by changing the leg geometry. The leg geometry is optimised by determining the leg height and the number of thermocouples, leading to maximisation of electric output power or efficiency at given operating conditions. Therefore, there is interdependence between the optimal leg geometry and the electrical load resistance  $R_L$  for a TEG. Hodes [23] presented a method to compute the leg geometry (number and height) that maximises the electric output power and  $\eta_{\text{TEG}}$  with negligible or finite electrical contact resistance at TEG interconnects. If a TEG has a low number of legs, the energy conversion is low, because the  $R_L$  is not sufficient to obtain an adequate high voltage. Inversely, if a TEG has too many legs, the total equivalent resistance of the TEG will increase and relatively high Joule losses will occur in the TEG when the load is supplied.

There is an optimal solution also for the leg length. If the leg is long, the electric output power is limited due to the increase in the internal resistance of the leg that limits the electric current. Conversely, a short leg will behave as a good thermal conductor that reduces the temperatures between its ends; hence, even though the

internal electrical resistance will be low, the electric output power will not be significant and the electric conversion efficiency will be low [9].

Lavric et al. [57] demonstrated that the electric output power is influenced by the effects above mentioned (a reduction of the leg length leads to a reduction of the electrical resistance; an increase of the leg length leads to the higher temperature difference across the TEG). If the geometric parameters of the TEG (leg length, semiconductor pair number and the base area ratio of semiconductor columns to TEG) are optimised, the electric output power and the thermoelectric conversion efficiency are considerably improved. Such an improvement is also reported in [58]. The first step was to consider the electric output power as the objective function and the inputs were the geometric parameters. The electrical output power values were about 269, 314, 338, and 893% higher than the values of the initial design. The second step was to consider the TEG conversion efficiency  $\eta_{\text{TEG}}$  as the objective function. A  $\eta_{\text{TEG}}$  rise is obtained for the optimal design at the same time with an important reduction of  $P$ . Finally, the third step was to use multi-objective optimization to improve both  $P$  and  $\eta_{\text{TEG}}$ , simultaneously.

Two dimensionless parameters influence the maximisation of the electric output power and the conversion efficiency of TEG [35]:

- slenderness ratio, which is a geometric parameter:

$$x = \frac{S_P \cdot (L_P)^{-1}}{S_N \cdot (L_N)^{-1}} \quad (31)$$

- external load parameter:

$$y = \frac{R_L}{L_N \cdot (\sigma_N \cdot S_N)^{-1}} \quad (32)$$

The thermal efficiency of the TEG can be improved while decreasing the slenderness ratio for large external load parameters. Yilbas and Sahin [35] obtained high conversion efficiency for the slenderness ratio  $0 < x < 1$  in the case of all the external load parameters.

Zhang et al. [55] propose a design method of thermoelectric elements segmentation of TEG, considering their length as the first design parameter. The optimal length ratio, referring to the highest values of the maximum electric output power, and the thermoelectric conversion efficiency are influenced by thermoelectric materials, leg geometry and heat transfer characteristics. Zhang et al. [59] proposed two new parameters, namely, the power factor associated with the electric output power, and the efficiency factor associated with the thermoelectric conversion efficiency. These new parameters are useful for obtaining the optimum temperature range of each segment:

$$(ZJ)_P = \alpha^2 \cdot \sigma \cdot (1 + m \cdot k)^{-2} \quad (33)$$

$$(ZJ)_\eta = Z \cdot (1 + m \cdot k)^{-1} \quad (34)$$

considering that the thermoelectric materials of the TEG legs have the same physical transport properties ( $\alpha_P = -\alpha_N$ ;  $\sigma_P = \sigma_N$ ;  $k_P = k_N$ ) and  $m$  is a variable factor that depends on the leg cross-sectional area, and on the heat transfer coefficients on both TEG sides.

### 2.5.2.2 Heat transfer enhancement at the hot and cold sides

The fins attached to the heat transfer surfaces are very important for enhancing the heat transfer at the hot and cold sides. One interface is between the heat sink and the TEG cold side, and the other interface is between the heat source and the TEG hot side.

An increment of the fin height and fin number results when the electric output power of the TEG rises [60]. An optimal connection between the height and the number of fins to provide the maximum net electric output power is obtained in Jang et al. [60]. The heat transfer increases when the fin number is higher and the fin height rises, due to the extension of the heat transfer area. However, when the height of the fin increases over a given value, the change in the output electrical power becomes less significant. Borcuch et al. [61] investigated the effect of hot side heat exchanger design on the operating parameters of a TEG. Furthermore, the heat sink connected to the TEG device must be thermally matched with the TEG to maximise the electric output power and voltage. In this case, the thermal interface losses are practically negligible, that means  $T_{\text{heat sink}} \cong T_c$  and  $T_{\text{heat source}} \cong T_h$ .

To maximise the output voltages of TEG, a big number of thermocouples are necessary, and their total thermal resistance must be equal to the thermal resistance of the heat sink. The reduced thermal resistance of the TEG decreases very much the temperature difference [62].

The thermal resistance of the heat sink is:

$$R_{\text{hs}} = \frac{T_{\text{heat sink}} - T_{\text{amb}}}{\dot{Q}_h} \quad (35)$$

where  $\dot{Q}_h$  the heat flow is given by Eq. (18) through the TEG,  $T_{\text{heat sink}}$  is the heat sink temperature, and  $T_{\text{amb}}$  is the environmental temperature.

The thermal resistance and thermal conductance of TEG are linked with each other by an inverse ratio as:

$$R = \frac{1}{K} \quad (36)$$

The thermal energy through the TEG is written as:

$$\dot{Q}_h = \frac{T_{\text{heat source}} - T_{\text{amb}}}{R_{\text{tot}}} \quad (37)$$

considering that  $R_{\text{hs}}$  and  $R$  are connected in series with the total resistance  $R_{\text{tot}} = R + R_{\text{hs}}$ , and  $T_{\text{heat source}}$  is the heat source temperature.

The following cases may be considered:

- If  $\frac{R}{R_{\text{hs}}} < 1$ , a big heat source-to-environment  $\Delta T$  occurs across the heat sink and  $\Delta T_{\text{TEG}} < \Delta T_{\text{heat sink}}$ . In this case, a reduction of the thermoelectric conversion efficiency  $\eta_{\text{TEG}}$  is observed, leading to a reduction of the TEG electric output power.
- If  $\frac{R}{R_{\text{hs}}} > 1$ , a big heat source-to-environment  $\Delta T$  occurs across the TEG and  $\Delta T_{\text{TEG}} > \Delta T_{\text{heat sink}}$ . In this case, an increment of the  $\eta_{\text{TEG}}$  is observed, leading to a limited electric output power.

- When  $\frac{R}{R_{hs}} = 1$ , the electric output power has a peak. In this case, the lengths and cross sections of thermoelectric legs are adapted,  $R = R_{hs}$  and  $\Delta T$  is equally divided between the heat sink and the TEG.

Also, when the heat sinks are attached to both sides of the TEG, the total thermal resistance (thermal interfaces resistances and thermal resistances of the heat sinks) is equal to the  $R_{TEG}$  for maximum electric output power [62]. The contact resistance decreases the electric output power by decreasing  $\Delta T$  across the TEG. Furthermore, the thermal contact resistance between the TEG and the heat sink or heat source is decreased to reduce the contact effect [63].

Astrain et al. [64] demonstrated the significance of decreasing the thermal resistance between the heat source and the hot side of the TEG, as well as the cold side of TEG and the environment. The numerical model assesses the TEG performance, taking into account the heat exchangers attached on both sides of the TEG, the heat source, as well as the heat sink. The results obtained show a good accuracy of the model. The results demonstrated that increasing by 10% the thermal resistances of both heat exchangers, the electric output power is improved by 8%. Martínez et al. [65] optimised the heat exchangers fixed on both sides of a TEG to maximise the electric output power. They have concluded that the thermal resistances of the heat exchangers are very important for TEG design. Zhou et al. [66] studied the heat transfer features of a TEG device. The heat transfer intensification on the cold side of the TEG leads to a significant reduction of the temperature and thermal resistance on this side, and implicitly a rise of the electric output power of the TEG device. Furthermore, Zhou et al. [66] highlighted that the refrigerant which flows by heat exchangers produce higher net powers than conventional heat sink with fins. An in-depth review of the heat sink for TEG and parameters affecting TEG performance is presented in [26].

The refrigeration system of the TEG has been assessed by Aranguren et al. [30]. This system consists of a multi-channel heat exchanger attached to the cold side of the TEG, another heat exchanger used to decrease the refrigerant temperature, the pump to circulate the refrigerant, and the connecting pipes. A numerical model has been implemented to compute the total thermal resistance and the power consumption in the system components. In this model, all system elements have been included to obtain an accurate analysis. The combination of computational and experimental results shows that the system configuration leading to the maximum net power is different with respect to the configuration resulting in the lowest total thermal resistance.

### 3. Applications using thermoelectrics in the power generation mode

The favourable characteristics of the thermoelectric devices promote the development of standalone TEGs for energy harvesting in a wide range of applications (**Figure 8**) as military, aerospace (e.g., powering spacecraft), biological systems (e.g., to power implanted pacemakers) and other applications (e.g., power for wristwatches or mobile communications) [67]. The key element to improve the energy conversion efficiency of TEG is the effect of waste heat recovery. Waste heat represents the heat produced by machines (e.g., exhaust pipes from automobiles), industrial processes (e.g., cooling towers, burnt solid waste and radioactive wastes), electrical equipment (e.g., kerosene lamps) and the human body. For various TEG applications (e.g., waste thermal power recovery using TEGs and powering of



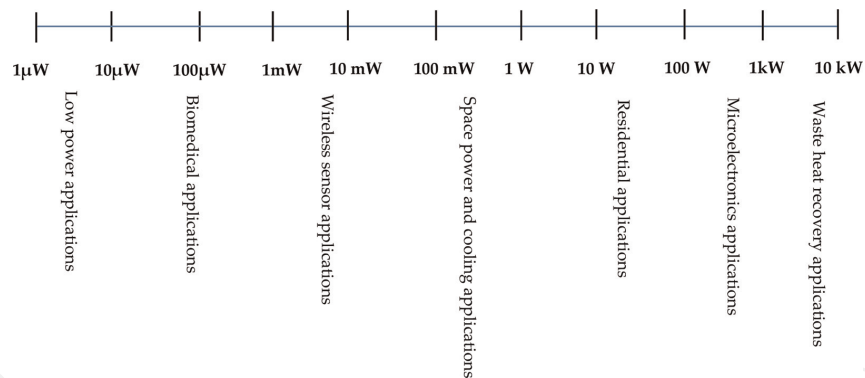


**Figure 8.**  
*Energy conversion applications.*

wireless sensors by TEGs) even if  $\Delta T$  is restricted, the available heat is higher than the capacity of the harvesters. In this case, the heat source delivers a constant heat flow rate at a constant  $\Delta T$ . Low  $\eta_{\text{TEGmax}}$  in such applications does not mean low TEG performance [32].

### 3.1 Low-power generation for thermoelectric harvesting

#### 3.1.1 Microelectronic applications

The TEG devices are especially suitable for waste heat harvesting for low-power generation to supply electric energy for microelectronic applications. Wearable TEGs harvest heat generated by the body to generate electricity. For this reason, it is possible to use waste human body heat to power a TEG watch device. In this case, the wristwatch can capture the thermoelectric energy. Now, body-attached TEGs are commercially available products including watches operated by body temperature and thin film devices. Some manufacturers produce and commercialise wristwatches with an efficiency about 0.1% at 300 mV open circuit voltage from 1.5 K temperature drop and 22  $\mu\text{W}$  of electric output power under of TEG normal operation. A thermo-clock wristwatch produces a voltage of 640 mV and gives a power of 13.8  $\mu\text{W}$  for each  $^{\circ}\text{C}$  of temperature difference. A wristwatch with 1040 thermoelements generates in the same conditions at about 200 mV [25]. The wearable TEG performance is affected by the utilisation of the free air convection cooling on the cold side of TEG, the low operating temperature difference between the body and environment, as well as the demand for systems that are thin and lightweight, being practical for long-term usage [68].

Furthermore, various microelectronic devices, like wireless sensor networks, mobile devices (e.g., mp3 player, smartphones and iPod), and biomedical devices are developed. The thermoelectric energy harvesters are microelectronic devices made of inorganic thermoelectric materials, at different dimensions, with a lifetime of about 5 years [69] and electric output powers are cardiac pacemakers ( $P = 70 \div 100 \mu\text{W}$ ) [70], pulse oximeter ( $P = 100 \mu\text{W}$ ) [71], wireless communication ( $P \sim 3 \text{ mW}$ ) [72], electrocardiography (ECG)/electroencephalography (EEG)/electromyography (EMG) with  $P = 60 \div 200 \mu\text{W}$  [73], EEG headband ( $P = 2 \div 2.5 \text{ mW}$ ) [74], ECG system ( $P \sim 0.5 \mu\text{W}$ ) [75], Hearing aid ( $P \sim 1 \mu\text{W}$ ) [76] and Wireless EEG [77]. Together with the progress of flexible thermoelectric materials (both organic and inorganic materials), flexible TEGs system benefits from special attention. The flexible thermoelectric materials and maximum electric output power of various TEG systems are reported in [44].

For these microelectronic devices, standard batteries are used. These batteries are made of various inorganic materials (like nickel, zinc, lithium, lead, mercury,

sulphuric acid and cadmium) that are not friendly for the human body. In this case, the body-attached TEGs could be an alternative solution because the materials used are non-toxic [36].

A TEG to be applied in a network of body sensors has been presented in [78]. In this case, the device has been fixed in a body zone, where the maximum body heat has been obtained and also maximum energy. This equipment is capable of storing about 100  $\mu\text{W}$  on the battery, leading to an output voltage of 2.4 V. Another TEG has been designed to be used on the wrist [79]. The output voltage of the device was 150 mV under normal conditions and an electric output power of 0.3 nW.

### 3.1.2 TEG as a thermal energy sensor

Thermal energy sensors (like heat-flux sensors, infrared sensors, power ultrasound effect sensors, fluid-flow sensors and water condensation detectors) are used to convert heat flow rates into electrical signals by a TEG system [36].

The heat-flux sensors are used to evaluate the thermoelectric properties of micro-TEGs. In this case, the generated power and the thermoelectric conversion efficiency are measured with high accuracy [80]. The electrical signal generated by the heat-flux sensor is proportional to the heat flow rate applied to the sensor surface. The convective heat flow rate is measured from the temperature difference between two sides of a thermal resistive element plate placed across the flow of heat. The heat radiated from the mass is absorbed by the infrared sensor (IR) and the temperature increase leads to the generation of the Seebeck voltage. The thermoelectric IR sensor operates in a range from 7 to 14  $\mu\text{m}$  [69].

## 3.2 High-power generation for thermoelectric harvesting

About 70% of energy in the world is wasted as heat and is released into the environment with a significant influence on global warming [81]. The waste heat energy released into the environment is one of the most significant sources of clean, fuel-free and cheap energy available. The unfavourable effects of global warming can be diminished using the TEG system by harvesting waste heat from residential, industrial and commercial fields [36].

TEG is substantially used to recover waste heat in different applications ranging from  $\mu\text{W}$  to MW. Different waste heat sources and temperature ranges for thermoelectric energy harvesting are shown in **Table 2** [69].

### 3.2.1 Automotive applications

The automotive industry is considered as the most attractive sector in which TEGs are used to recover the lost heat. Various leading automobile manufacturers develop TEGs ( $P \sim 1 \text{ kW}$ ) for waste recovery to reduce the costs of the fuel for their vehicles [82]. It has been demonstrated that vehicles (the gasoline vehicle and hybrid electric vehicles) have inefficient internal combustion engines. This can be observed in the Sankey diagram depicted in [83], which presents the energy flow direction of an internal combustion engine. The fuel combustion is used in a proportion of 25% for vehicle operation, 30% is lost into the coolant and 40% is lost as waste heat with exhaust gases. In this case, the TEG technology could be an option to recuperate the waste heat energy for gasoline vehicles and hybrid electric vehicles. A significant power conversion could be achieved by combining cooling system losses with the heat recovery from automobile exhausts. The use of TEG systems with an energy conversion of 5% would raise the electrical energy in a vehicle by 6% (5% from exhaust gases and 1% from the cooling system) [25].



Temperature ranges, °C	Temperature, °C	Waste heat sources
High temperature (>650°C)	650–760	Aluminium refining furnaces
	760–815	Copper reverberatory furnace
	760–110	Copper refining furnace
	620–730	Cement kiln Hydrogen plants
Medium temperature (230–650°C)	315–600	Reciprocating engine exhausts
	425–650	Catalytic crackers
	425–650	Annealing furnace cooling systems
Low temperature (230–650°C)	32–55	Cooling water
	27–50	Air compressors
	27–88	Forming Dies and pumps

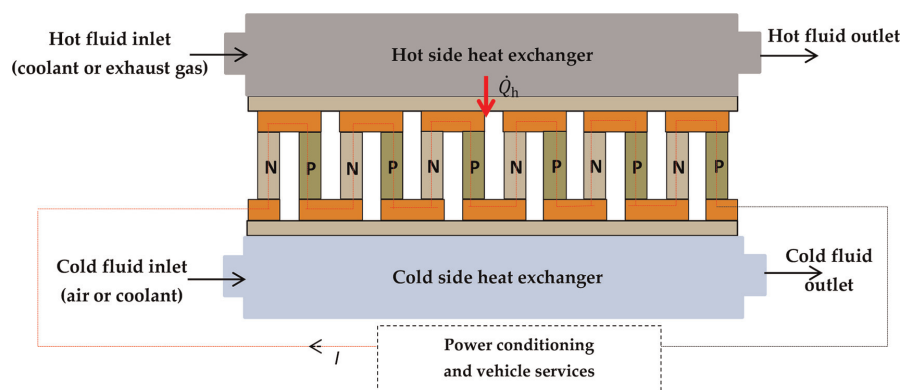
**Table 2.**

*Different waste heat sources and temperature ranges for thermoelectric harvesting technology.*

A TEG with  $ZT = 1.25$  and efficiency of 10%, can recover about 35–40% of the power from the exhaust gas where the power generated can help to increase the efficiency to up 16% [84]. The components where TEGs could be attached in a vehicle are the exhaust system and the radiators. In this case, the amount of waste heat is decreased and exhaust temperatures are reduced. These aspects require more efficiency from the TEG device. Furthermore, the design of such power conversion system takes into account various heat exchangers mounted on the TEG device. These systems have a lifecycle from 10 to 30 years and the materials accumulated on their surfaces from the exhaust gas, air or coolant represent a major concern in order to not damage their proper operation [85]. Important testing is helpful to confirm the reliability of TEG systems in automotive applications. Furthermore, the design requires knowing the maximum electric output power and conversion efficiency from TEG systems [37].

The main components of the automotive TEG that considers waste heat like their energy source are one heat exchanger which takes heat from engine coolant and the exhaust gases and release it to the hot side of the TEG; the TEG system; one heat exchanger which takes the heat from the TEG and releases it to the coolant or to the air; the electrical power conditioning and the interface unit to supply the electric output power of the TEG system to the automobile electric system (**Figure 9**). Supplementary at these components, there are secondary components (e.g., the electronic unit, the electric pump, sensors system, valves, fans and so on) depending on the vehicle design and application type [85].

Thacher et al. [86] carried out the feasibility of the TEG system installed in the exhaust pipe in a light truck by connecting a series of 16 TEG modules. The

**Figure 9.**

*The main components of an automotive TEG system.*

experimental results showed good performance of the system at high speeds. Hsiao et al. [87] carried out an analytical and experimental assessment of the waste heat recovery system from an automobile engine. The results showed better performance by attaching TEGs to the exhaust pipe than to the radiators. Hsu et al. [88] introduced a heat exchanger with 8 TEGs and 8 air-cooled heat sink assemblies, obtaining a maximum power of 44 W. An application to recover waste heat has been developed by Hsu et al. [89], for a system consisting of 24 TEGs used to convert heat from the exhaust pipe of a vehicle to electrical energy. The results show a temperature increase at the hot side  $T_h$  from 323 to 403 K and a load resistance of 23–30  $\Omega$  to harvest the waste heat for the system. Tian et al. [90] theoretically analysed the performance between a segmented TEG ( $\text{Bi}_2\text{Te}_3$  used in low-temperature region and Skutterudite in high-temperature areas) used to recover exhaust waste heat from a diesel engine and traditional TEG. They found that a segmented TEG is suitable for large temperature difference and a high-temperature heat source, and has a higher potential for waste heat recovery compared to the traditional device. Meng et al. [91] addressed the automobile performance when applying TEG in exhaust waste heat recovery. The results showed that the effects of the different properties and the heat loss to the environmental gas on performance are considerable.

The conversion efficiency for the TEG system could be in the range of 5–10% [83]. The researchers' attention is focused on the development of new thermoelectric materials that offer improved energy conversion efficiency and a working temperature range more significant than for internal combustion engines. It is planned by 2020, about 90% of cars in the USA to have mounted TEGs for their cooling equipment, thus replacing the air conditioning systems. In this case, an amount of 5% of daily average gasoline consumption would be saved and a significant reduction of greenhouse gas emissions would be obtained [25].

To recover waste heat from the exhaust gas of engines, the research efforts of manufacturers focused on different solutions to compete in the production of ever-cleaner cars. Even if the cost of the bismuth telluride is relatively high, the technical feasibility of TEGs for the automobile industry is widely demonstrated, making it very attractive. The goal of the manufacturers is to develop TEG systems with automated production and low-cost thermoelectric materials [29].

### 3.2.2 Air applications

#### 3.2.2.1 Space vehicle applications

A considerable amount of heat is released into the atmosphere from space vehicles (turbine engines from helicopters and aircraft jet engines) [29]. To obtain a significant reduction of the gas pollutant into the environment, it is necessary a remarkable reduction of electricity consumption and utilisation of the available energy in these types of vehicles. Implicitly, their operating costs are reduced [25].

To power these space vehicles, TEG systems are used (e.g., on fixed-wing aircraft). The backup TEG is a type of static thermoelectric energy harvesting system with a significant temperature difference across the TEG around 100°C [92].

TEG for energy harvesting uses the available temperature gradient and collects sufficient energy to power up an energy wireless sensor node (WSN) to be autonomous. This WSN is used for health monitoring systems (HMS) in an aircraft structure. The main components of a WSN are the energy source and the wireless sensor unit. An in-depth review of WSN mechanisms and applications is presented in [10].

A TEG energy harvesting captures enough energy for a wireless sensor. One side of the TEG is fixed directly to the fuselage and the other side is attached to a

phase-change material (PCM) heat storage unit to obtain a temperature difference during take-off and landing (**Figure 10**). PCM is considered an essential element for the heat storage unit because it can maximise the  $\Delta T$  of the TEG system to solve the low TEG conversion efficiency [93]. In this case, the electrical energy is generated [94]. Water is an adequate PCM for heat storage. The temperature difference across the TEG is obtained from the slow changing temperature of the heat storage unit and the rapidly changing temperature of the aircraft fuselage. A lot of energy is produced during the PC, through latent heat [95, 96].

An application of  $\text{Bi}_2\text{Te}_3$  modules on turbine nozzles has been addressed in [97]. Even though the electric power that can be harvested may be significant, the weight of the cold exchanger is still excessive for the specific application.

Future applications in aircraft may be envisioned in locations in which there are hot and cold heat flows, especially with the use of light thermoelectric materials. However, one of the main issues remains the weight of the heat exchangers [29].

### 3.2.2.2 Spacecraft applications

The radioisotope thermoelectric generators (RTGs) are a solid and highly reliable source of electrical energy to power space vehicles being capable of operating in vacuum and to resist at high vibrations [98, 99]. RTGs are used to power space vehicles for distant NASA space expeditions (e.g., several years or several decades) where sunlight is not enough to supply solar panels [29]. The natural radioactive decay of plutonium-238 releases huge amounts of heat, which is suitable for utilisation in RTGs to convert it into electricity. The thermoelectric materials used the thermocouples of the RTGs are adequate for high temperature considering that the heat source temperature is about  $1000^\circ\text{C}$  [100]. These semiconductor materials can be silicon germanium (Si Ge), lead tin telluride (PbSnTe), tellurides of antimony, germanium, and silver (TAGS) and lead telluride (PbTe).

### 3.2.3 Marine applications

Up to now, just a few surveys have been performed in the marine industry due to the lack of clear and stringent international rules at the global level. The marine transport has a significant influence on climate change because is a large amount of the greenhouse gas emissions [29]. The naval transport generates a wide amount of waste heat, used to provide thermal energy onboard and seldom electrical energy.

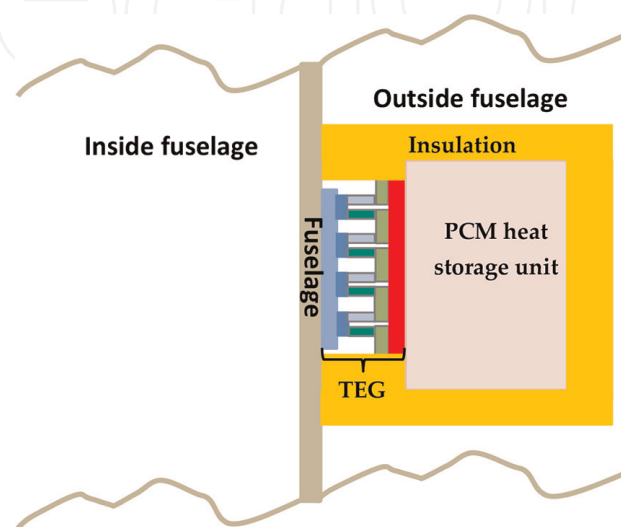


**Figure 10.**  
Schematic of the thermoelectric harvesting system in an aircraft.

The heat sources on the marine vessels are the main engine, lubrication oil cooler, an electrical generating unit, generator and incinerators. The utilisation of waste heat onboard is for heating heavy fuel oil and accommodation places, and for freshwater production. The main engine represents the principal source of waste heat. Board incinerators are used for burning the onboard waste instead to be thrown overboard to pollute the sea water. The incinerators are the most favourable TEG systems due to the availability of their high-temperature differences [101, 102].

The specialists' attention is focused on the future design and optimisation of the high-power density TEGs for the marine environment, as well as on the development of hybrid thermoelectric ships considered as green platforms for assessing the efficiency of TEGs [103].

### 3.2.4 Industrial applications

The industry is the field where most amounts of heat are emitted and released into the atmosphere in the form of flue gases and radiant heat energy with a negative impact to the environmental pollution (emissions of CO<sub>2</sub>). For this reason, thermoelectric harvesters are good candidates to recover waste heat from industries and convert it into useful power (e.g., to supply small sensing electronic device in a plant).

Utilisation of TEGs in the industrial field is beneficial from two points of view:

- in the industrial applications where recoverability of the waste heat by the conventional system (radiated heat energy) is very difficult to be done;
- in the industrial applications where the use of thermoelectric materials reduces the need for maintenance of the systems and the price of the electric power is low, even if the efficiency is low [29].

The results of a test carried out on a TEG system attached at a carburising furnace (made of 16 Bi<sub>2</sub>Te<sub>3</sub> modules and a heat exchanger) are indicated in [104]. The system harvested about 20% of the heat ( $P = 4$  kW). The maximum electrical output power generated by TEG has been approximately 214 W, leading to thermoelectric conversion efficiency 5%. Aranguren et al. [105] built a TEG prototype. The TEG has been attached at the exhaust of a combustion chamber, with 48 modules connected in series and two different kinds of finned heat sinks, heat exchangers and heat pipes. This TEG was used to recover waste heat from the combustion chamber. In this case, the main objective has been to maximise the electric output power generated by the TEG.

For this reason, the dissipation systems have been used on both sides of TEG. This prototype has obtained a 21.56 W of net power using about 100 W/m<sup>2</sup> from the exhaust gases of the combustion chamber. To recover the radiant heat from melted metal from the steelmaking industry, the TEG systems are also considered good candidates [29].

Furthermore, TEGs are useful for recovery of waste heat from the cement rotary kiln to generate electricity, considering that the rotary kiln is the main equipment used for large-scale industrial cement production [106]. The performance of this hybrid Bi<sub>2</sub>Te<sub>3</sub> and PbTe thermoelectric heat recovery system is obtained by developing a mathematical model. In this case, about 211 kW electrical output power and 3283 kW heat loss are saved by using a thermoelectric waste heat energy recovery system. The contribution of TEG is about 2%.



The electric output power evaluation of a TEG system attached to an industrial thermal oil heater is presented in Barma et al. [107]. The impact of different design and flow parameters has been assessed to maximise the electrical output power. The estimated annual electrical power generation from the proposed system was about 181,209 kWh. The thermal efficiency of the TEG based on recently developed thermoelectric materials (N-type hot forged  $\text{Bi}_2\text{Te}_3$  and P-type  $(\text{Bi,Sb})_2\text{Te}_3$  used for the temperature range of 300–573 K) was enhanced up to 8.18%.

### 3.2.5 Residential applications

In residential applications, TEGs can be feasible where the heat is transferred from high temperatures to a reduced temperature heat source, and then is released into the environment. In addition, TEG can be also feasible when thermal energy is accessible in high amounts without additional costs. Types of residential applications where TEG systems could be mounted are with TEGs attached to domestic boilers, TEGs attached to stoves, as well as TEGs attached to solar systems [27].

#### 3.2.5.1 TEGs connected to the local heating boiler

The heating boilers for residential applications provide central heating and hot water. These heating boilers are highly used in the places where the winter season with temperatures under  $0^\circ\text{C}$  has a long duration and the heating is necessary for all this period. The fuels used by these heating boilers can be biomass (e.g., firewood, wood pellets, wood chips) or renewable resources that provide a lower carbon footprint compared to fossil fuels [108, 109]. In spite of higher pollution, some residential applications use fossil fuel-fired boilers (boilers supplied with natural gas) due to their low maintenance [27]. Furthermore, the fuel combustion is high, providing combustion temperatures bigger than  $1000^\circ\text{C}$ .

Instead, the heating boilers contain enhanced heat transfer surfaces due to the fins, and inside them combustion takes place at over  $500^\circ\text{C}$ . The heat obtained is used for water heating at temperatures fewer than  $80^\circ\text{C}$ . By considering that some thermoelectric materials are available for high temperatures, TEGs are very suitable for this type of equipment. In this case, high-temperature differences are obtained if the TEG cold side is mounted to the water heating side and the TEG hot side is mounted to the combustion chamber of the heat exchanger. The TEG system attached to the heating boiler must provide an electric output power  $P = 30\div 70\text{W}$ , as this boiler has to generate the power necessary to supply the auxiliary devices and the pumps of the heating system. These boilers are widely reviewed in [27].

#### 3.2.5.2 TEGs attached to the stove

At the global level, over than 14% of the population is still living without electricity access according to the Energy Access Outlook 2017 [110]. To deliver a small amount of electricity by using power plants to this population could be very costly. Grid connection of villages in remote areas supposes to take into account the cost of the connection of the new power lines to the grid and the distribution cost on long distances [29]. Also, traditional biomass stoves ('threestone fires', 'built-in stoves' or 'mud-stoves') have a reduced thermal efficiency due to incomplete fuel burning, and a lot of the heat generated is wasted through the exhausts. Furthermore, the indoor air quality is very poor related to the utilisation of biomass fuels with a negative impact on the users' health (e.g., lung diseases, respiratory tract infections, cardiac problems, stroke, eye diseases, tuberculosis and cancer) [111].

Considering that most of the stoves are used in the rural areas in remote locations away from the grid, where the income of the population is very low, the solutions with such hybrid systems (TEGs attached to stoves) must be as inexpensive as possible. These hybrid systems must be very reliable and durable, taking into account this vital problem [111]. In this case, a TEG device attached to the stove equipment used for heating and food preparation could be an attractive option. The biomass stoves-powered TEG uses heat exchangers on both sides of TEG, as well as a power management system. The internal temperatures of a stove are bigger than  $600^{\circ}\text{C}$ , while most commercial TEGs can operate continuously at temperatures higher than  $250^{\circ}\text{C}$ , so that an appropriate hot side temperature could be obtained. To obtain a maximum electric output power, the cold side temperature must be very low. In this case, the cold sink dissipates a big amount of heat maintaining its low temperature [112].

According to the literature survey, various extensive reviews about stove-attached TEG systems have been presented [27, 29, 111–114]. A good option is the utilisation of the stoves using water as the cooling medium of the TEG to produce the maximum electric output power. The electrical output power decreases if the number of the TEGs is increased on the same heat sink. Such a hybrid system is suitable for complete combustion. The overall efficiency could be substantially improved [111].

### 3.2.5.3 TEGs attached to the solar systems

Solar TEG (STEG) systems, PV systems and concentrating solar power plants can generate electricity by using the solar heat. A STEG is composed of a TEG system sandwiched between a solar absorber and a heat sink as shown in **Figure 11**. The solar flux is absorbed by the solar absorber and concentrated into one point. Then, the heat is transferred through TEG by using a pipeline, and is partially

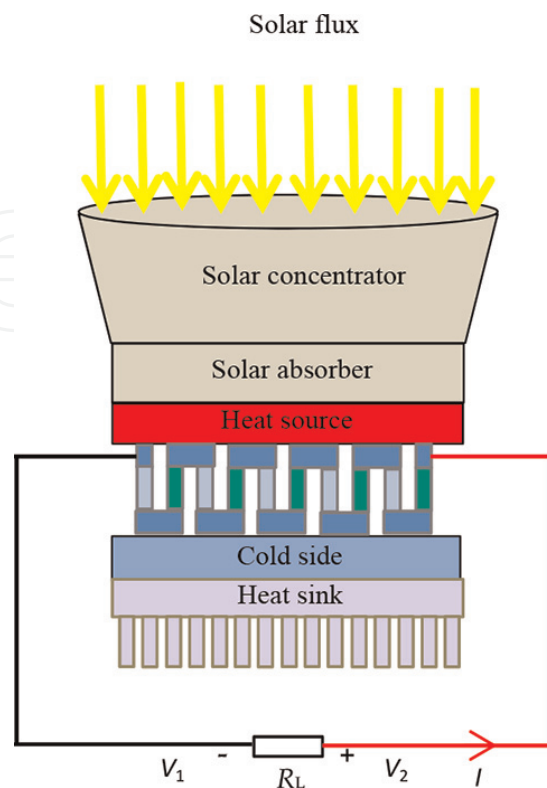


**Figure 11.**  
*Components of STEG system.*



converted into electrical power by the TEG. A heat sink rejects the excess heat at the cold junction of the TEG to keep a proper  $\Delta T$  across the TEG [115].

Due to the development of the thermoelectric materials, a solar TEG with an incident flux of  $100 \text{ kW/m}^2$  and a hot side temperature of  $1000^\circ\text{C}$  could obtain 15.9% conversion efficiency. The solar TEG is very attractive for standalone power conversion. The efficiency of a solar TEG depends on both the efficiency with which sunlight is absorbed and converted into heat, and the TEG efficiency  $\eta_{\text{TEG}}$ . Furthermore, the total efficiency of a solar TEG is also influenced by the heat lost from the surface. The efficiency of solar TEG systems is relatively small due to the low Carnot efficiency provoked by the reduced temperature difference across the TEG and the reduced  $ZT$  [116]. Its improvement needs to rise temperature differences and to develop new materials with high  $ZT$  like nanostructured and complex bulk materials (e.g., a device with  $ZT = 2$  and a temperature of  $1500^\circ\text{C}$  would lead to obtain a conversion efficiency about 30.6%) [117]. According to the literature survey, both residential and commercial applications gain much more interest in the regions of incident solar radiation of solar TEGs. This can be explained by the fact that most of the heat released at the cold side of the TEG can be used for domestic hot water and space heating [115].

### 3.2.6 Grid integration of TEG

Most TEG applications have been designed for autonomous operation within a local system. Of course, the TEG output may be connected to different types of loads. In general, a TEG can be seen as a renewable energy power generation source that supplies an autonomous system or a grid-connected system. To be suitable for grid connection, the TEG needs an appropriate power conditioning system. This power conditioning system has to be a power electronic system, with specific regulation capabilities, different with respect to the ones used for solar photovoltaic and wind power systems [114], because the TEG operating conditions are different with respect to the other renewable energy sources. Molina et al. [118] proposed a control strategy to perform energy conversion from DC to AC output voltage, which maintains the operation of the thermoelectric device at the MPP. In the same proposal, active and reactive power controls are addressed by using a dedicated power conditioning system.

## 4. Conclusions

This chapter has addressed the structures and applications of TEGs in various contexts. It has emerged that the TEG is a viable solution for energy harvesting, able to supply electrical loads in relatively low-power applications. The TEG efficiency is also typically low. Thereby, the advantages of using TEG have to be found in the characteristics of specific applications in which there is a significantly high-temperature difference across the TEG system, and other solutions with higher efficiency cannot be applied because of various limitations. These limitations may be the relatively high temperatures for the materials adopted, the strict requirements on the system to be used (regarding the type of operation, emissions of pollutants, the position of the device during operation or noise). In these cases, TEGs may be fully competitive with the other solutions.

In particular, the use of TEGs is entirely consistent with the provision of green energy through energy harvesting from even small temperature differences. Some low-power applications have been identified on electronic circuits, sensors, waste heat recovery, residential energy harvesting and automotive systems. In other

applications to enhance the efficiency of the systems for energy production with a higher power, the efficiency increase is still somewhat limited to consider that an investment in TEG integration may be profitable. Nevertheless, there is a growing interest in the potential of thermoelectric applications. For the future, faster development of TEG solutions can be expected in a broader range of green energy applications. This development depends on improvements in the TEG technology, better information on the TEG characteristics, and the testing of new solutions aimed at promoting better integration in the energy production systems.

## Nomenclature

### Acronyms

COP	coefficient of performance
DC	direct current
ECG	electrocardiography
EEG	electroencephalography
EMG	electromyography
HMS	health monitoring systems
IR	infrared sensor
MPP	maximum power point
MPPT	maximum power point tracking
PANI	polyaniline
PA	polyamide
PCM	phase-change material
PC	phase-change
PEDOT	poly
RF	radio-frequency
RTG	radioisotope thermoelectric generator
STEG	solar thermoelectric generator
TEG	thermoelectric generator
WSN	wireless sensor node

### Symbols

$E$	electric field ( $V \cdot m^{-1}$ )
$I$	electrical current (A)
$J$	current density ( $A \cdot m^{-2}$ )
$\bar{J}$	relative current density ( $A \cdot m^{-2}$ )
$k$	thermal conductivity ( $W \cdot m^{-1} \cdot K^{-1}$ )
$K$	thermal conductance ( $W \cdot K^{-1}$ )
$L$	length (m)
$m$	resistance ratio
$n$	number of thermoelectric couples
$P$	electric power (W)
$\dot{Q}$	heat flow rate (W)
$R$	resistance ( $\Omega$ )
$S$	cross-section ( $m^2$ )
$t$	temperature ( $^{\circ}C$ )
$T$	absolute temperature (K)
$\Delta T$	temperature difference (K)

$\nabla T$	temperature gradient (K)
$u$	compatibility factor
$V$	voltage (V)
$x$	slenderness ratio
$y$	external load parameter
$Z$	thermoelectric figure-of-merit ( $W \cdot K^{-1}$ )
$ZT$	dimensionless figure-of-merit

### Greek symbols

$\alpha$	Seebeck coefficient ( $V \cdot K^{-1}$ )
$\varepsilon$	fraction of waste heat passed through the thermoelectric couples (efficiency)
$\eta$	(efficiency)
$\mu$	Thomson coefficient ( $V \cdot K^{-1}$ )
$\pi$	Peltier coefficient (V)
$\rho$	electrical resistivity ( $\Omega \cdot m$ )
$\sigma$	electrical conductivity ( $S \cdot m^{-1}$ )

### Subscripts

a	contact
amb	(ambient)
c	cold side
C	Carnot
h	hot side
hs	heat sink
L	load
N	N-type semiconductor
P	P-type semiconductor
max	maximum
r	reduced
t	thermal
tot	total


### Author details

Diana Enescu

Department of Electronics, Telecommunications and Energy, Valahia University of Targoviste, Targoviste, Romania

\*Address all correspondence to: [diana.enescu@valahia.ro](mailto:diana.enescu@valahia.ro)

### IntechOpen

© 2019 The Author(s). Licensee IntechOpen. This chapter is distributed under the terms of the Creative Commons Attribution License (<http://creativecommons.org/licenses/by/3.0>), which permits unrestricted use, distribution, and reproduction in any medium, provided the original work is properly cited. 

## References

- [1] Roundy S, Steingart D, Frechette L, Wright P, Rabaey J. Power sources for wireless sensor networks. In: 1st European Workshop on Wireless Sensor Networks Berlin; 2004
- [2] Vullers RJM, van Schaijk R, Doms I, Van Hoof C, Mertens R. Micropower energy harvesting. *Solid-State Electronics*. 2009;53(7):684-693. DOI: 10.1016/j.sse.2008.12.011
- [3] Steingart D, Roundy S, Wright PK, Evans JW. Micropower materials development for wireless sensor networks. *MRS Bulletin*. 2008;33(4): 408-409. DOI: 10.1557/mrs2008.81
- [4] Sim ZW. Radio frequency energy harvesting for embedded sensor networks in the natural environment [MS Degree thesis]. Manchester, England; 2011
- [5] Snyder GJ. Thermoelectric energy harvesting. In: Priya S, Inman DJ, editors. *Energy Harvesting Technologies*. Boston, MA, USA: Springer; 2009. pp. 325-336. DOI: 10.1007/978-0-387-76464-1\_11
- [6] Cheng TC, Cheng CH, Huang ZZ, Liao GC. Development of an energy-saving module via combination of solar cells and thermoelectric coolers for green building applications. *Energy*. 2011;36(1):133-140. DOI: 10.1016/j.energy.2010.10.061
- [7] Wang CC, Hung CI, Chen WH. Design of heat sink for improving the performance of thermoelectric generator using two-stage optimization. *Energy*. 2012;39:236-245. DOI: 10.1016/j.energy.2012.01.025
- [8] Camacho-Medina P, Olivares-Robles PA, Vargas-Almeida A, Solorio-Ordaz A. Maximum power of thermally and electrically coupled thermoelectric generators. *Entropy*. 2014;16:2890-2903. DOI: 10.3390/e16052890
- [9] Brownell E, Hodes M. Optimal design of thermoelectric generators embedded in a thermal resistance network. *IEEE Transactions on Components, Packaging and Manufacturing Technology*. 2014;4(4): 612-621. DOI: 10.1109/TCPMT.2013.2295169
- [10] Shaikh FK, Zeadally S. Energy harvesting in wireless sensor networks: A comprehensive review. *Renewable and Sustainable Energy Reviews*. 2017; 55:1041-1054. DOI: 10.1016/j.rser.2015.11.010
- [11] Simons RE, Ellsworth MJ, Chu RC. An assessment of module cooling enhancement with thermoelectric coolers. *Journal of Heat Transfer-Transaction ASME*. 2005;127:76-84. DOI: 10.1115/1.1852496
- [12] Cheng TC, Cheng CH, Huang ZZ, Liao GC. Development of an energy-saving module via combination of solar cells and thermoelectric coolers for green building applications. *Energy*. 2011;36:133-140. DOI: 10.1016/j.energy.2010.10.061
- [13] Enescu D. Thermoelectric refrigeration principle. In: Patricia Aranguren P, editor. *Bringing Thermoelectricity into Reality*, INTECH Publishing; 2018. pp. 221-246. DOI: 10.5772/intechopen.75439
- [14] Kong LB, Li T, Hng HH, Boey F, Zhang T, Li S. *Waste Energy Harvesting. Mechanical and Thermal Energies*. Verlag Berlin Heidelberg, Germany: Springer; 2014. 592 p. DOI: 10.1007/978-3-642-54634-1
- [15] Champier D, Bedecarrats JP, Kousksou T, Rivaletto M, Strub F, Pignolet P. Study of a TE (thermoelectric) generator incorporated in a multifunction wood stove. *Energy*.



2011;**36**:1518-1526. DOI: 10.1016/j.energy.2011.01.01

[16] Champier D, Bedecarrats JP, Rivaletto M, Strub F. Thermoelectric power generation from biomass cook stoves. *Energy*. 2010;**35**:935-942. DOI: 10.1016/j.energy.2009.07.015

[17] Marciá-Barber E. Thermoelectric Materials. Advances and Applications. NY, USA: Taylor & Francis Group, Pan Stanford. 2015. 350 p. ISBN 978-981-4463-53-9

[18] Neeli G, Behara DK, Kumar MK. State of the art review on thermoelectric materials. *International Journal of Science and Research*. 2016;**5**:1833-1844. ISSN:2319-7064

[19] Goupil C, Seifert W, Zabrocki K, Müller E, Snyder GF. Thermodynamics of thermoelectric phenomena and applications. *Entropy*. 2011;**13**:1481-1517. DOI: 10.3390/e13081481

[20] Agrawal M. Basics of Irreversible Thermodynamics. Stanford, CA, USA: Stanford University; 2005

[21] DiSalvo FJ. Thermoelectric cooling and power generation. *Science*. 1999; **285**(5248):703-706. DOI: 10.1126/science.285.5428.703

[22] von Lukowicz M, Abbe E, Schmiel T, Tajmar M. Thermoelectric generators on satellites—An approach for waste heat recovery in space. *Energies*. 2016; **9**(7):1-14. DOI: 10.3390/en9070541

[23] Hodes M. Optimal pellet geometries for thermoelectric power generation. *IEEE Transactions on Components and Packaging*. 2010;**33**(2):307-318. DOI: 10.1109/TCAPT.2009.2039934

[24] Orr B, Akbarzadeh A, Mochizuki M, Singh R. A review of car waste heat recovery systems utilising thermoelectric generators and heat pipes. *Applied Thermal Engineering*.

2016;**101**:490-495. DOI: 10.1016/j.applthermaleng.2015.10.081

[25] Ando Junior OH, Maran ALO, Henao NC. A review of the development and applications of thermoelectric microgenerators for energy harvesting. *Renewable and Sustainable Energy Reviews*. 2018;**91**:376-393. DOI: 10.1016/j.rser.2018.03.052

[26] Elghool A, Basrawi F, Ibrahim TK, Habib K, Ibrahim H, Idris DMND. A review on heat sink for thermo-electric power generation: Classifications and parameters affecting performance. *Energy Conversion and Management*. 2017;**134**:260-277. DOI: 10.1016/j.enconman.2016.12.046

[27] Kütt L, Millar J, Karttunen A, Lehtonen M, Karppinen M. Thermoelectric applications for energy harvesting in domestic applications and micro-production units. Part I: Thermoelectric concepts, domestic boilers and biomass stoves. *Renewable and Sustainable Energy Reviews*. 2018;**98**:519-544. DOI: 10.1016/j.rser.2017.03.051

[28] Thermoelectric power generation: Properties, application and novel TCAD simulation. In: Proceedings of the IEEE International Conference on Power Electronics and Applications; 30 August–1 September 2011. Birmingham, UK: IEEE; 2011. pp. 1-10

[29] Champier D. Thermoelectric generators: A review of applications. *Energy Conversion and Management*. 2017;**140**:167-181. DOI: 10.1016/j.enconman.2017.02.070

[30] Aranguren P, Astrain D, Pérez MG. Computational and experimental study of a complete heat dissipation system using water as heat carrier placed on a thermoelectric generator. *Energy*. 2014; **74**:346-358. DOI: 10.1016/j.energy.2014.06.094

[31] Rowe DM. Handbook of Thermoelectrics. Introduction.



Boca Raton, FL, USA: CRC Press, Taylor & Francis Group; 1995. 720 p. ISBN: 9780849301469

[32] Kiziroglou ME, Yeatman EM. Materials and techniques for energy harvesting. In: Kilner JA, Skinner SJ, Irvine SJC, Edwards PP, editors. Woodhead Publishing Series in Energy, Functional Materials for Sustainable Energy Applications. Cambridge, UK: Woodhead Publishing; 2012. pp. 541-572. DOI: 10.1533/9780857096371.4.539

[33] Ali H, Sahin AZ, Yilbas BS. Thermodynamic analysis of a thermoelectric power generator in relation to geometric configuration device pins. *Energy Conversion and Management*. 2014;**78**:634-640. DOI: 10.1016/j.enconman.2013.11.029

[34] Crane DT, Jackson GS. Optimization of cross flow heat exchangers for thermoelectric waste heat recovery. *Energy Conversion and Management*. 2004;**45**(9-10):1565-1582. DOI: 10.1016/j.enconman.2003.09.003

[35] Yilbas BS, Sahin AZ. Thermoelectric device and optimum external load parameter and slenderness ratio. *Energy*. 2010;**35**(12):5380-5384. DOI: 10.1016/j.energy.2010.07.019

[36] Aswal DK, Basu R, Singh A. Key issues in development of thermoelectric power generators: High figure-of-merit materials and their highly conducting interfaces with metallic interconnects. *Energy Conversion and Management*. 2016;**114**:50-67. DOI: 10.1016/j.enconman.2016.01.065

[37] Niu X, Yu J, Wang S. Experimental study on low-temperature waste heat thermoelectric generator. *Journal of Power Sources*. 2009;**188**:621-626. DOI: 10.1016/j.jpowsour.2008.12.067

[38] Sahin AZ, Yilbas BS. The thermoelement as thermoelectric power generator: Effect of leg geometry on the

efficiency and power generation. *Energy Conversion and Management*. 2013;**65**:26-32. DOI: 10.1016/j.enconman.2012.07.020

[39] Stobart R, Milner D. The potential for thermo-electric regeneration of energy in vehicles. *SAE Technical Papers*. 2009;**1**:1-14. DOI: 10.4271/2009-01-1333

[40] Rosenberg Y, Gelbstein Y, Dariel MP. Phase separation and thermoelectric properties of the Pb<sub>0.25</sub>Sn<sub>0.25</sub>Ge<sub>0.5</sub>Te compound. *Journal of Alloys and Compounds*. 2012;**526**:31-38. DOI: 10.1016/j.jallcom.2012.02.099

[41] Gelbstein Y, Davidow J. Highly efficient functional GexPb<sub>1-x</sub>Te based thermoelectric alloys. *Physical Chemistry Chemical Physics*. 2014;**16**:20120-20126. DOI: 10.1039/C4CP02399D

[42] Kirievsky K, Shlimovich M, Fuks D, Gelbstein Y. An ab-initio study of the thermoelectric enhancement potential in nano-grained TiNiSn. *Physical Chemistry Chemical Physics*. 2014;**16**:20023-20029. DOI: 10.1039/c4cp02868f

[43] Gelbstein Y, Tunbridge J, Dixon R, Reece MJ, Ning HP, Gilchrist R, et al. Physical, mechanical and structural properties of highly efficient nanostructured n- and p-silicides for practical thermoelectric applications. *Journal of Electronic Materials*. 2014;**43**:1703-1711. DOI: 10.1007/s11664-013-2848-9

[44] Zhou M, Al-Furjan MSH, Zou J, Liu W. A review on heat and mechanical energy harvesting from human—Principles, prototypes and perspectives. *Renewable and Sustainable Energy Reviews*. 2018;**82**:3582-3609. DOI: 10.1016/j.rser.2017.10.102

[45] Caillat T, Fleurial JP, Snyder GJ, Borshchevsky A. Development of high

efficiency segmented thermoelectric uncouples. In: Proceedings of the 20th International Conference on Thermoelectrics (ICT2001); 8-11 June 2001; Beijing, China: IEEE; 2001. pp. 282-285. DOI: 10.1109/ICT.2001.979888

[46] El-Genk MS, Saber HH. High efficiency segmented thermoelectric uncouple for operation between 973 and 300 K. *Energy Conversion and Management*. 2003;**44**(7):1069-1088. DOI: 10.1016/S0196-8904(02)00109-7

[47] Snyder GJ. Application of the compatibility factor to the design of segmented and cascaded thermoelectric generators. *Applied Physics Letters*. 2004;**84**(13):2436-2438

[48] Snyder GJ, Ursell T. Thermoelectric efficiency and compatibility. *Physical Review Letters*. 2003;**91**(14):148301. DOI: 10.1103/PhysRevLett.91.148301

[49] Ngan PH, Christensen DV, Snyder GJ, et al. Towards high efficiency segmented thermoelectric uncouples. *Physica Status Solidi*. 2014;**211**(1):9-17. DOI: 10.1002/pssa.201330155

[50] Hung LT, Van Nong N, Han L, Bjørk R, Ngan PH, Holgate TC, et al. Segmented thermoelectric oxide-based module for high-temperature waste heat harvesting. *Energy Technology*. 2015;**3**:1143-1151. DOI: 10.1002/ente.201500176

[51] Ali H, Yilbas BS, Al-Sulaiman FA. Segmented thermoelectric generator: Influence of pin shape configuration on the device performance. *Energy*. 2016;**111**:439-452. DOI: 10.1016/j.energy.2016.06.003

[52] Ali H, Yilbas BS, Al-Sharafi A. Segmented thermoelectric generator: exponential area variation in leg. *International Journal of Energy*

Research. 2018;**42**:477-489. DOI: 10.1002/er.3825

[53] Vikhor LN, Anatyshuk LI. Generator modules of segmented thermoelements. *Energy Conversion and Management*. 2009;**50**:2366-2372. DOI: 10.1016/j.enconman.2009.05.020

[54] Zhang Q, Liao J, Tang Y, Gu M, Ming C, Qiu P, et al. Realizing a thermoelectric conversion efficiency of 12% in bismuth telluride/skutterudite segmented modules through full-parameter optimization and energy-loss minimized integration. *Energy & Environmental Science*. 2017;**10**:956-963. DOI: 10.1039/C7EE00447H

[55] Zhang G, Fan L, Niu Z, Jiao K, Diao H, Du Q, et al. A comprehensive design method for segmented thermoelectric generator. *Energy Conversion and Management*. 2015;**106**:510-519. DOI: 10.1016/j.enconman.2015.09.068

[56] Min G, Rowe DM. Optimization of thermoelectric module geometry for 'waste heat' electric power generation. *Journal of Power Sources*. 1992;**38**(3):253-259. DOI: 10.1016/0378-7753(92)80114-Q

[57] Lavric ED. Sensitivity analysis of thermoelectric module performance with respect to geometry. *Energy*. 2010;**21**:133-138. DOI: 10.3303/CET1021023

[58] Meng JH, Zhang XX, Wang XD. Multi-objective and multi-parameter optimization of a thermoelectric generator module. *Energy*. 2014;**71**:367-376. DOI: 10.1016/j.energy.2014.04.082

[59] Zhang G, Jiao K, Niu Z, Diao H, Du Q, Tian H, et al. Power and efficiency factors for comprehensive evaluation of thermoelectric generator materials. *International Journal of Heat and Mass Transfer*. 2016;**93**:1034-1037. DOI:

10.1016/j.ijheatmasstransfer.2015.10.051

[60] Jang JY, Tsai YC, Wu CW. A study of 3-D numerical simulation and comparison with experimental results on turbulent flow of venting flue gas using thermoelectric generator modules and plate fin heat sink. *Energy*. 2013;**53**: 270-281

[61] Borcuch M, Musiał M, Gumuła S, Sztekler K, Wojciechowski K. Analysis of the fins geometry of a hot-side heat exchanger on the performance parameters of a thermoelectric generation system. *Applied Thermal Engineering*. 2017;**127**:1355-1363. DOI: 10.1016/j.applthermaleng.2017.08.147

[62] Bierschenk JL. Optimized thermoelectrics for energy harvesting applications. In: Priya S, Inman DJ, editors. *Energy Harvesting Technologies*. USA: Springer; 2009. pp. 337-351. DOI: 10.1007/978-0-387-76464-1\_12

[63] Liang G, Zhou J, Huang X. Analytical model of parallel thermoelectric generator. *Applied Energy*. 2011;**88**(12):5193-5199. DOI: 10.1016/j.apenergy.2011.07.041

[64] Astrain D, Vián JG, Martínez A, Rodríguez A. Study of the influence of heat exchangers' thermal resistances on a thermoelectric generation system. *Energy*. 2010;**35**(2):602-612. DOI: 10.1016/j.energy.2009.10.031

[65] Martínez A, Vián JG, Astrain D, Rodríguez A, Berrio I. Optimization of the heat exchangers of a thermoelectric generation system. *Journal of Electronic Materials*. 2010;**39**(9):1463-1468. DOI: 10.1007/s11664-010-1291-4

[66] Zhou ZG, Zhu DS, Wu HX, Zhang HS. Modeling, experimental study on the heat transfer characteristics of thermoelectric generator. *Journal of*

*Thermal Science*. 2013;**22**(1):48-54. DOI: 10.1007/s11630-013-0591-4

[67] Riffat SB, Ma X. Thermoelectrics: A review of present and potential applications. *Applied Thermal Engineering*. 2003;**23**(8):913-935. DOI: 10.1016/S1359-4311(03)00012-7

[68] Settaluri KT, Lo H, Ram RJ. Thin thermoelectric generator system for body energy harvesting. *Journal of Electronic Materials*. 2012;**41**(6): 984-988. DOI: 10.1007/s11664-011-1834-3

[69] Zeb K, Ali SM, Khan B, Mehmood CA, Tareen N, Din W, et al. A survey on waste heat recovery: Electric power generation and potential prospects within Pakistan. *Renewable and Sustainable Energy Reviews*. 2017;**75**: 1142-1155. DOI: 10.1016/j.rser.2016.11.096

[70] Watkins C, Shen B, Venkatasubramanian R. Low-grade-heat energy harvesting using superlattice thermoelectrics for applications in implantable medical devices and sensors. In: *Proceedings of the 24th International Conference on Thermoelectrics (ICT 2005)*; 19-23 June; Clemson, SC, USA: IEEE; 2005. pp. 265-267. DOI: 10.1109/ICT.2005.1519934

[71] Torfs T, Leonov V, Van Hoof C, Gyselinckx B. Body-heat powered autonomous pulse oximeter. In: *Proceedings of the 5th IEEE Conference on Sensors*; 22-25 October 2006; Daegu, South Korea: IEEE; 2007. pp. 427-430. DOI: 10.1109/ICSENS.2007.355497

[72] Mateu L, Codrea C, Lucas N, Pollak M, Spies P. Human body energy harvesting thermogenerator for sensing applications. In: *Proceedings of the IEEE International Conference on Sensor Technologies and Applications (SENSORCOMM 2007)*; 14-20 October 2007; Valencia, Spain: IEEE; 2007.



pp. 366-372. DOI: 10.1109/  
SENSORCOMM.2007.4394949

[73] Zhang Y, Zhang F, Shakhsher Y, Silver JD, Klinefelter A, Nagaraju M, et al. A batteryless 19  $\mu$ W MICS/ISM-band energy harvesting body sensor node SoC for ExG applications. *IEEE Journal of Solid-State Circuits*. 2013; **48**(1):199-213. DOI: 10.1109/JSSC.2012.2221217

[74] Torfs T, Leonov V, Yazicioglu RF, Merken P, Van Hoof C, Vullers RJ, et al. Wearable autonomous wireless electroencephalography system fully powered by human body heat. In: *Proceedings of the IEEE International Conference on Sensors*; 26-29 October 2008; Lecce, Italy: IEEE; 2008. pp. 1269-1272. DOI: 10.1109/ICSENS.2008.4716675

[75] Leonov V, Torfs T, Van Hoof C, Vullers RJ. Smart wireless sensors integrated in clothing: An electrocardiography system in a shirt powered using human body heat. *Sensors & Transducers Journal*. 2009; **107**(8):165. ISSN: 1726-5479

[76] Lay-Ekuakille A, Vendramin G, Trotta A, Mazzotta G. Thermoelectric generator design based on power from body heat for biomedical autonomous devices. In: *Proceedings of IEEE international workshop on medical measurements and applications*; 29-30 May 2009; Cetraro, Italy: IEEE; 2009. pp. 1-4. DOI: 10.1109/MEMEA.2009.5167942

[77] Carmo JP, Gonçalves LM, Correia JH. Thermoelectric microconverter for energy harvesting systems. *IEEE Transactions on Industrial Electronics*. 2010; **57**(3):861-867. DOI: 10.1109/TIE.2009.2034686

[78] Gyselinckx B, Van Hoof C, Ryckaert J, Yazicioglu RF, Fiorini P, Leonov V. Human++: Autonomous wireless sensors for body area networks. In: *Custom Integrated Circuits Conference*,

San José, CA, 18–21 September 2005. IEEE; 2006. pp. 13-19

[79] Wang Z, Leonov V, Fiorini P, Van Hoof C. Realization of a wearable miniaturized thermoelectric generator for human body applications. *Sensors and Actuators, A: Physical*. 2009; **156**(1): 95-102. DOI: 10.1016/j.sna.2009.02.028

[80] Beretta D, Massetti M, Lanzani G, Caironi M. Thermoelectric characterization of flexible micro-thermoelectric generators. *The Review of Scientific Instruments*. 2017; **88**(1): 015103. DOI: 10.1063/1.4973417

[81] Zevenhovena R, Beyeneb A. The relative contribution of waste heat from power plants to global warming. *Energy*. 2011; **36**:3754-3762. DOI: 10.1016/j.energy.2010.10.010

[82] Elsheikh MM, Shnawah DA, Sabri MFM, Said SBM, Hassan MH, Bashir MBA, et al. A review on thermoelectric renewable energy: Principle parameters that affect their performance. *Renewable and Sustainable Energy Reviews*. 2014; **30**:337-355. DOI: 10.1016/j.rser.2013.10.027

[83] Yu C, Chau KT. Thermoelectric automotive waste heat energy recovery using maximum power point tracking. *Energy Conversion and Management*. 2009; **50**(6):1506-1512. DOI: 10.1016/j.enconman.2009.02.015

[84] Yu S, Du Q, Diao H, Shu G, Jiao K. Start-up modes of thermoelectric generator based on vehicle exhaust waste heat recovery. *Applied Energy*. 2015; **138**:276-290

[85] Yang J, Stabler FR. Automotive applications of thermoelectric materials. *Journal of Electronic Materials*. 2009; **38**(7):1245-1251. DOI: 10.1007/s11664-009-0680-z

[86] Thacher EF, Helenbrook BT, Karri KA, Richter CJ. Testing of an

- automobile exhaust thermoelectric generator in a light truck. Proceedings of the Institution of Mechanical Engineers, Part D: Journal of Automobile Engineering. 2007;**221**(1): 95-107. DOI: 10.1243/09544070JAUTO51
- [87] Hsiao YY, Chang WC, Chen SL. A mathematic model of thermoelectric module with applications on waste heat recovery from automobile engine. Energy. 2010;**35**(3):1447-1454. DOI: 10.1016/j.energy.2009.11.030
- [88] Hsu CT, Yao DJ, Ye KJ, Yu B. Renewable energy of waste heat recovery system for automobiles. Journal of Renewable and Sustainable Energy. 2010;**2**:013105. DOI: 10.1063/1.3289832
- [89] Hsu CT, Huang GH, Chu HS, Yu B, Yao DJ. Experiments and simulations on low-temperature waste heat harvesting system by thermoelectric power generators. Applied Energy. 2011;**88**(4): 1291-1297. DOI: 10.1016/j.apenergy.2010.10.005
- [90] Tian H, Sun X, Jia Q, Liang X, Shu G, Wang X. Comparison and parameter optimization of a segmented thermoelectric generator by using the high temperature exhaust of a diesel engine. Energy. 2015;**84**:121-130. DOI: 10.1016/j.energy.2015.02.063
- [91] Meng JH, Wang XD, Chen WH. Performance investigation and design optimization of a thermoelectric generator applied in automobile exhaust waste heat recovery. Energy Conversion and Management. 2016;**120**:71-80. DOI: 10.1016/j.enconman.2016.04.080
- [92] Janak L, Ancik Z, Vetiska J, Hadas Z. Thermoelectric generator based on MEMS module as an electric power backup in aerospace applications. Materials Today: Proceedings. 2015;**2**: 865-870. DOI: 10.1016/j.matpr.2015.05.112
- [93] Elefsiniotis A, Samson D, Becker T, Schmid U. Investigation of the performance of thermoelectric energy harvesters under real flight conditions. Journal of Electronic Materials. 2013; **42**(7):2301-2305. DOI: 10.1007/s11664-012-2411-0
- [94] Samson D, Otterpohl T, Kluge M, Schmid U, Becker T. Aircraft-specific thermoelectric generator module. Journal of Electronic Materials. 2010; **39**(9):2092-2095. DOI: 10.1007/s11664-009-0997-7
- [95] Samson D, Kluge M, Becker T, Schmid U. Energy harvesting for autonomous wireless sensor nodes in aircraft. Procedia Engineering. 2010;**5**: 1160-1163. DOI: 10.1016/j.proeng.2010.09.317
- [96] Elefsiniotis A, Kiziroglou ME, Wright SW, Toh TT, Mitcheson PD, Becker T, et al. Performance evaluation of a thermoelectric energy harvesting device using various phase change materials. Journal of Physics: Conference Series;**476**:1-5. DOI: 10.1088/1742-6596/476/1/012020
- [97] Kousksou T, Bedecarrats J-P, Champier D, Pignolet P, Brillet C. Numerical study of thermoelectric power generation for an helicopter conical nozzle. Journal of Power Sources. 2011;**196**:4026-4032. DOI: 10.1016/j.jpowsour.2010.12.015
- [98] Abelson RD. Space missions and applications. In: Rowe DM, editor. Thermoelectrics Handbook Macro to Nano. Boca Raton, Fl, USA: CRC Press, Taylor & Francis Group; 2006. pp. 56-1-56-26. ISBN 0-8493-2264-2
- [99] Fleurial JP, Caillat T, Nersisyan BJ, Ewell RC, Woerner DF, Carr GC, et al. Thermoelectrics: From space power systems to terrestrial waste heat recovery applications. In: 2nd Thermoelectrics Applications Workshop. 2011



- [100] LeBlanc S. Thermoelectric generators: Linking material properties and systems engineering for waste heat recovery applications. *Sustainable Materials and Technologies*. 2014;**1-2**: 26-35. DOI: 10.1016/j.susmat.2014.11.002
- [101] Kristiansen NR, Nielsen HK. Potential for usage of thermoelectric generators on ships. *Journal of Electronic Materials*. 2010;**39**(9): 1746-1749. DOI: 10.1007/s11664-010-1189-1
- [102] Kristiansen N, Snyder G, Nielsen H, Rosendahl L. Waste heat recovery from a marine waste incinerator using a thermoelectric generator. *Journal of Electronic Materials*. 2012;**41**(6): 1024-1029. DOI: 10.1007/s11664-012-2009-6
- [103] Wallace TT. Development of marine thermoelectric heat recovery systems. In: *The 2nd Thermoelectrics Applications Workshop* 5 January 2011
- [104] Kaibe H, Makino K, Kajihara T, Fujimoto S, Hachiuma H. Thermoelectric generating system attached to a carburizing furnace at Komatsu Ltd., Awazu Plant. *AIP Conference Proceedings*. 2012;**1449**: 524-527. DOI: 10.1063/1.4731609
- [105] Aranguren P, Astrain D, Rodriguez A, Martinez A. Experimental investigation of the applicability of a thermoelectric generator to recover waste heat from a combustion chamber. *Applied Energy*. 2015;**152**:121-130. DOI: 10.1016/j.apenergy.2015.04.077
- [106] Luo Q, Li P, Cai L, Zhou P, Tang D, Zhai P, et al. A thermoelectric waste-heat recovery system for Portland cement rotary kilns. *Journal of Electronic Materials*. 2015;**44**(6): 1750-1762. DOI: 10.1007/s11664-014-3543-1
- [107] Barma MC, Riaz M, Saidur R, Long BD. Estimation of thermoelectric power generation by recovering waste heat from Biomass fired thermal oil heater. *Energy Conversion and Management*. 2015;**98**:303-313. DOI: 10.1016/j.enconman.2015.03.103
- [108] Moser W, Friedl G, Haslinger W, Hofbauer H. Small-scale pellet boiler with thermoelectric generator. In: *Proceedings of the 25th International Conference on Thermoelectrics*. 6-10 August 2006; Vienna Austria: IEEE; 2007. pp. 349-353. DOI: 10.1109/ICT.2006.331221
- [109] Thomson A, Liddell C. The suitability of wood pellet heating for domestic households: A review of literature. *Renewable and Sustainable Energy Reviews*. 2015;**42**:1362-1369. DOI: 10.1016/j.rser.2014.11.009
- [110] International Energy Agency [Internet]. Available from: <https://www.iea.org/energyaccess/database/> [Accessed: June 28, 2018]
- [111] Najjar YSH, Kseibi MM. Thermoelectric stoves for poor deprived regions – A review. *Renewable and Sustainable Energy Reviews*. 2017;**80**: 597-602. DOI: 10.1016/j.rser.2017.05.211
- [112] Gao HB, Huang GH, Li HJ, Qu ZG, Zhang YZ. Development of stove-powered thermoelectric generators: A review. *Applied Thermal Engineering*. 2016;**96**:297-310. DOI: 10.1016/j.applthermaleng.2015.11.032
- [113] Deasy MJ, O'Shaughnessy SM, Archer L, Robinson AJ. Electricity generation from a biomass cook stove with MPPT power management and passive liquid cooling. *Energy for Sustainable Development*. 2018;**43**: 162-172. DOI: 10.1016/j.esd.2018.01.004
- [114] Date A, Date A, Dixon C, Akbarzadeh A. Progress of

thermoelectric power generation  
systems: Prospect for small to medium  
scale power generation. *Renewable and  
Sustainable Energy Reviews*. 2014;**33**:  
371-381. DOI: 10.1016/j.rser.2014.01.081

[115] Kraemer D, McEnaney K, Chiesa  
M, Chen G. Modeling and optimization  
of solar thermoelectric generators for  
terrestrial applications. *Solar Energy*.  
2012;**86**(5):1338-1350. DOI: 10.1016/j.  
solener.2012.01.025

[116] Olsen ML, Warren EL, Parilla PA,  
Toberer ES, Kennedy CE, Snyder GJ,  
et al. A high-temperature, high-  
efficiency solar thermoelectric  
generator prototype. *Energy Procedia*.  
2014;**49**:1460-1469. DOI: 10.1016/j.  
egypro.2014.03.155

[117] Baranowski LL, Snyder GJ, Toberer  
ES. Concentrated solar thermoelectric  
generators. *Energy & Environmental  
Science*. 2012;**5**:9055-9067. DOI:  
10.1039/C2EE22248E

[118] Molina MG, Juanicó LE, Rinalde  
GF. Design of innovative power  
conditioning system for the grid  
integration of thermoelectric  
generators. *International Journal of  
Hydrogen Energy*. 2012;**37**(13):  
10057-10063. DOI: 10.1016/j.  
ijhydene.2012.01.177